

Deep Learning Based 3D Segmentation: A Survey

Yong He^a, Hongshan Yu^{a,*}, Xiaoyan Liu^a, Zhengeng Yang^a, Wei Sun^a, Saeed Anwar^b and Ajmal Mian^c

^aHunan University, Lushan South Rd., Yuelu Dist., Changsha, 410082, Hunan, China

^bThe Australian National University, Acton, Canberra, 2600, ACT, Australia

^cUniversity of Western Australia, 35 Stirling Hwy, Perth, 6009, WA, Australia

ARTICLE INFO

Keywords:

Computer vision
Deep learning
Deep neural network
3D semantic segmentation
3D instance segmentation
3D part segmentation

ABSTRACT

3D segmentation is a fundamental and challenging problem in computer vision with applications in autonomous driving and robotics. It has received significant attention from the computer vision, graphics and machine learning communities. Conventional methods for 3D segmentation, based on hand-crafted features and machine learning classifiers, lack generalization ability. Driven by their success in 2D computer vision, deep learning techniques have recently become the tool of choice for 3D segmentation tasks. This has led to an influx of many methods in the literature that have been evaluated on different benchmark datasets. Whereas survey papers on RGB-D and point cloud segmentation exist, there is a lack of a recent in-depth survey that covers all 3D data modalities and application domains. This paper fills the gap and comprehensively surveys the recent progress in deep learning-based 3D segmentation techniques. We cover over 220 works from the last six years, analyze their strengths and limitations, and discuss their competitive results on benchmark datasets. The survey provides a summary of the most commonly used pipelines and finally highlights promising research directions for the future.

1. Introduction

Segmentation of 3D scenes is a fundamental and challenging problem in computer vision as well as computer graphics. The objective of 3D segmentation is to build computational techniques that predict the fine-grained labels of objects in a 3D scene for a wide range of applications, such as autonomous driving, mobile robots, industrial control, and augmented and virtual reality. As illustrated in Figure 1, 3D segmentation can be divided into semantic, instance and part segmentation. Semantic segmentation aims to predict object class labels such as tables and chairs. Instance segmentation additionally distinguishes between different instances of the same class labels, e.g., chair one and two. Part segmentation aims to further decompose instances into various components, such as the same chair's armrests, legs, and backrests. Semantic, instance, and part segmentation tasks show a progressive relationship in terms of semantic levels. Despite the difference in specific goals of three segmentation tasks, these tasks share a broader, unifying goal: they aim to segment 3D data into semantically meaningful regions based on certain criteria—whether it's by class, instance, part.

Compared to conventional single view 2D segmentation, 3D segmentation gives a more comprehensive understanding of a scene since 3D data (e.g., RGB-D, point cloud, voxel, mesh, 3D video) contain richer geometric, shape, and scale information with less background noise. Moreover, the representation of 3D data, for example, in the form of projected images, has more semantic information.

*Corresponding author

✉ h.yong@hnu.edu.cn (Y. He); yuhongshancn@hotmail.com (H. Yu);
xiaoyan.liu@hnu.edu.cn (X. Liu); yzg050215@163.com (Z. Yang);
david-sun@126.com (W. Sun); saeed.anwar@kfupm.edu.sa (S. Anwar);
ajmal.mian@uwa.edu.au (A. Mian)

ORCID(s): 0000-0003-2916-3068 (Y. He); 0000-0003-1973-6766 (H. Yu)

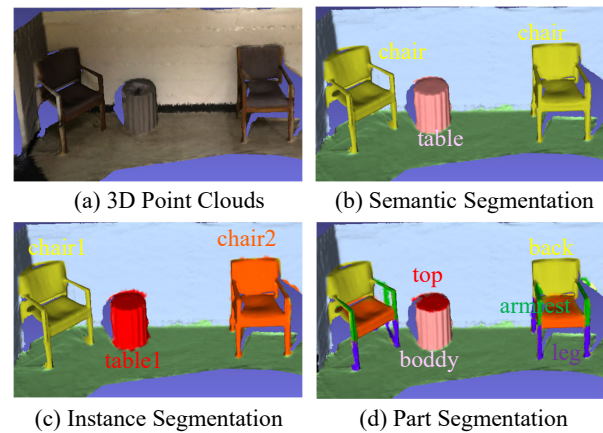


Fig. 1: The main three types of 3D segmentation are (b) 3D semantic segmentation, (c) 3D instance segmentation, and (d) 3D part segmentation on (a) 3D point clouds.

Recently, deep learning techniques have dominated many research areas, including computer vision and natural language processing. Motivated by its success in learning powerful features, deep learning for 3D segmentation has also attracted growing interest from the research community over the past decade. However, 3D deep learning methods still face many unsolved challenges. For example, the irregularity of point clouds makes it difficult to exploit local features, and converting them to high-resolution voxels has a substantial computational burden.

This paper comprehensively surveys recent progress in deep learning methods for 3D segmentation. It focuses on analyzing commonly used building blocks, convolutional kernels and complete architectures, pointing out the pros

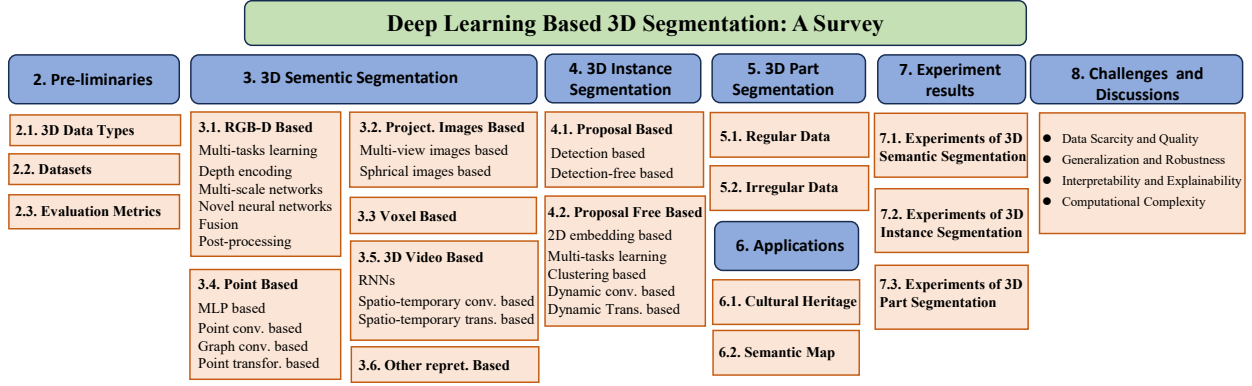


Fig. 2: Complete overview of the survey paper. Highlighting each section and its essential content.

and cons in each case. The survey covers over 180 representative articles published in the last six years. Although some notable 3D segmentation surveys have been released including RGB-D semantic segmentation [35], remote sensing imagery segmentation [222], point clouds segmentation [204], [44], [113], [6], [128], [67], these surveys do not comprehensively cover all 3D data types and typical application domains. Most importantly, these surveys do not focus on 3D segmentation but give a general survey of deep learning from point clouds [44], [113], [6], [128], [67]. Given the differences in domain knowledge required for semantic, instance, and part segmentation tasks in 3D segmentation, this paper reviews the deep learning techniques for each of these three segmentation tasks separately. Figure 2 shows the overview of the whole article. The contributions of this paper are summarized as follows:

- To the best of our knowledge, this is the first survey paper to comprehensively cover deep learning methods on 3D segmentation in computer vision, covering the most common 3D data representations, including RGB-D, projected images, voxels, point clouds, meshes, and 3D videos.
- This survey provides an in-depth analysis of the relative advantages and disadvantages of different 3D data segmentation methods. Unlike existing reviews, this survey focuses on deep learning methods designed specifically for 3D segmentation and discusses typical segmentation pipelines.
- Finally, this survey provides comprehensive comparisons of existing methods on several public benchmark 3D datasets, draws interesting conclusions, and identifies promising future research directions.

2. Pre-liminaries

This section introduces 3D data representations, popular 3D segmentation datasets, and evaluation metrics to help the reader easily navigate the rest of the survey.

2.1. 3D Data Types

With the rapid development of 3D sensors, different type of 3D data could be accessed easily. While raw data originate from different sensors they might be transformed into a common 3D data format. For instance, raw 3D data generated from depth camera, terrestrial LiDAR, and mobile LiDAR can be transformed into a common point cloud format that includes coordinates and other attributes (e.g. RGB and surface normal). We provide the details of the most common types of 3D data used in 3D segmentation, specifically for computer vision and 3D vision community, which are visually shown in Figure 3.

RGBD: is a type of 3D data that combines RGB (Red, Green, Blue) color information with depth (D) information. It is commonly represented as a pair of images: a standard RGB image capturing color information and a depth image capturing distance information from the camera to objects in the scene. RGB-D data is typically obtained using depth-sensing devices like Microsoft Kinect, Intel RealSense, or structured light cameras. These devices emit infrared light or use other depth-sensing techniques to measure the distance to objects in the scene, producing a depth map. RGB-D data is used for scene reconstruction and 3D modeling, object recognition and scene segmentation, and augmented reality and virtual reality. Some works refer to RGB-D data as 2.5D data, which indicates that it lies between traditional 2D images and complete 3D data. While RGB-D data may not represent a complete three-dimensional dataset in the conventional sense, its inclusion of depth information gives it some three-dimensional characteristics; here, we justify its classification as 3D data. RGB-D data can be transformed into point clouds, further integrating it into the 3D data framework.

Point Clouds: are collections of points in 3D space, where each point represents a specific position and may include additional attributes such as color and intensity. Point clouds are commonly used to describe the surfaces of objects or environments in a scene. Point cloud data can be obtained through various methods, including 3D scanning

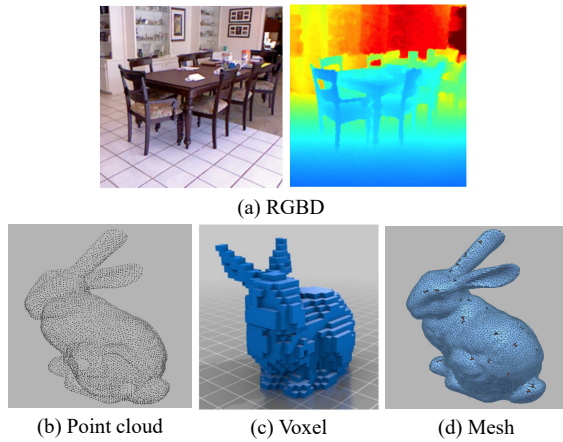


Fig. 3: The four types of 3D data are (a) RGBD, (b) Point cloud, (c) Voxel, and (d) Mesh.

with LiDAR sensors, structured light scanners, stereo vision systems, or photogrammetry techniques. Point clouds have many applications, including object identification and classification, environment mapping, localization, and obstacle detection in robotics and autonomous vehicles. Additionally, point clouds can be transformed into other 3D data formats such as voxels and meshes, enhancing their versatility in various applications.

Voxel: data represents three-dimensional objects or scenes using a regular grid of volumetric pixels called voxels. Each voxel represents a small volume element in three-dimensional space and can store various attributes such as color, density, or material properties. Voxel data is typically employed in medical imaging, computer graphics, physics simulations, and computational modeling.

Meshe: represent 3D objects or surfaces using a collection of vertices, edges, and faces, forming a network of interconnected triangles or polygons. Each vertex defines a point in 3D space, and each face consists of a set of vertices that define a surface. Computer graphics, animation, and simulation applications utilize Meshe. It can be obtained through 3D scanning, computer-aided design (CAD) modeling, or procedural generation. Mesh data is generally used in object segmentation, computer graphics and animation, and finite element analysis domains.

2.2. Datasets

Datasets are critical to train and test 3D segmentation algorithms using deep learning. However, privately gathering and annotating datasets is cumbersome and expensive as it needs domain expertise, high-quality sensors and processing equipment. Thus, building on public datasets is an ideal way to reduce costs. Following this way has another advantage for the community: it compares algorithms fairly. Table 1 summarizes some of the most popular and typical datasets concerning the sensor type, data size and format, scene class and annotation method.

These datasets are acquired for 3D semantic segmentation by different type of sensors, including RGB-D cameras [155], [156], [158], [62], [21], mobile laser scanner [148], [5], static terrestrial scanner [46] and unreal engine [10], [197] and other 3D scanners [2], [12]. Among these, the ones obtained from unreal engines are synthetic datasets [10], [197] that do not require expensive equipment or annotation time. These are also rich in categories and quantities of objects. Synthetic datasets have complete 360-degree 3D objects with no occlusion effects or noise compared to the real-world datasets, which are noisy and contain occlusions [155], [156], [158], [62], [21], [148], [5], [2], [46], [12]. For 3D instance segmentation, there are limited 3D datasets, such as ScanNet [21] and S3DIS [2]. These two datasets contain separate scans of real-world indoor scenes obtained by RGB-D cameras or Matterport. For 3D part segmentation, the Princeton Segmentation Benchmark (PSB) [14], COSEG [182] and ShapeNet [217] are three of the most popular datasets. Below, we introduce five famous segmentation datasets in detail, including S3DIS [2], ScanNet [21], Semantic3D [46], SemanticKITTI [12] and ShapeNet [217]. Some examples with annotation from these datasets are shown in Figure 4.

S3DIS: In this dataset, the complete point clouds are obtained without any manual intervention using the Matterport scanner. The dataset consists of 271 rooms belonging to six large-scale indoor scenes from three different buildings (a total of 6020 square meters). These areas mainly include offices, educational and exhibition spaces, conference rooms etc.

Semantic3D comprises around four billion 3D points acquired with static terrestrial laser scanners, covering up to $160 \times 240 \times 30$ meters in real-world 3D space. Point clouds belong to 8 classes (e.g., urban and rural) and contain 3D coordinates, RGB information, and intensity. Unlike 2D annotation strategies, 3D data labeling is readily amenable to over-segmentation, where each point is individually assigned to a class label.

SemanticKITTI is a large outdoor dataset containing detailed point-wise annotation of 28 classes. Building on the KITTI vision benchmark [39], SemanticKITTI contains annotations of all 22 sequences of this benchmark consisting of 43K scans. Moreover, the dataset contains labels for the complete horizontal 360 field-of-view of the rotating laser sensor.

ScanNet dataset is particularly valuable for research in scene understanding as its annotations contain estimated calibration parameters, camera poses, 3D surface reconstruction, textured meshes, dense object-level semantic segmentation, and CAD models. The dataset comprises annotated RGB-D scans of real-world environments. There are 2.5M RGB-D images in 1513 scans acquired in 707 distinct places. After RGB-D image processing, human intelligence tasks were annotated using the Amazon Mechanical Turk.

ShapeNet dataset has a novel scalable method for efficient and accurate geometric annotation of massive 3D

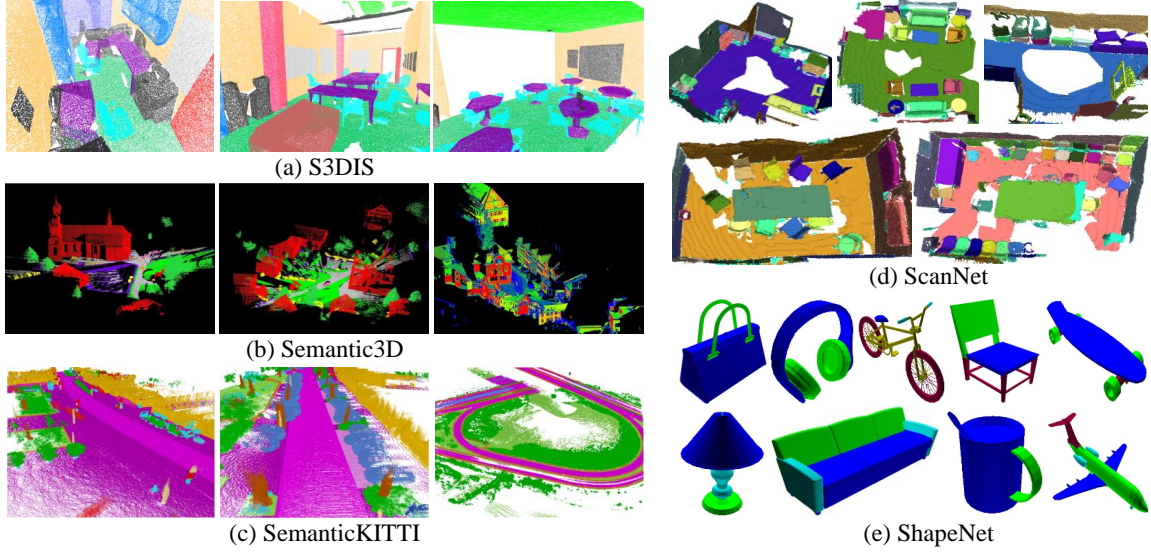


Fig. 4: Annotated examples from (a) S3DIS, (b) Semantic3D, (c) SemanticKITTI for 3D semantic segmentation, (d) ScanNet for 3D instance segmentation, and (e) ShapeNet for 3D part segmentation. See Table 1 for a summary of these datasets.

shape collections. The novel technical innovations explicitly model and lessen the human cost of the annotation effort. Researchers create detailed point-wise labeling of 31963 models in shape categories in ShapeNetCore and combine feature-based classifiers, point-to-point correspondences, and shape-to-shape similarities into a single CRF optimization over the network of shapes.

2.3. Evaluation Metrics

Different evaluation metrics can assert the validity and superiority of segmentation methods, including the execution time, memory footprint and accuracy. However, few authors provide detailed information about the execution time and memory footprint of their methods. This paper introduces the accuracy metrics mainly.

For 3D semantic segmentation, Overall Accuracy (OA), mean class Accuracy (mA) and mean class Intersection over Union (mIoU) are the most frequently used metrics to measure the accuracy of segmentation methods. For the sake of explanation, we assume that there are a total of K classes, and p_{ij} is the minimum unit (e.g., pixel, voxel, mesh, point) of class i implied to belong to class j . In other words, p_{ii} represents true positives, while p_{ij} and p_{ji} represent false positives and false negatives, respectively.

Overall Accuracy: is a straightforward metric that computes the ratio between the number of truly classified samples and the total number of samples.

$$OA = \frac{\sum_{i=0}^K p_{ii}}{\sum_{i=0}^K \sum_{j=0}^K p_{ij}}. \quad (1)$$

Mean Accuracy: is an extension of OA, computing OA in a per-class and then averaging over the total number of classes.

$$mA = \frac{1}{K+1} \sum_{i=0}^K \frac{p_{ii}}{\sum_{j=0}^K p_{ij}} \quad (2)$$

Mean Intersection over Union: is a standard metric for semantic segmentation. It computes the intersection ratio between ground truth and predicted value averaged over the total number of classes K .

$$mIoU = \frac{1}{K+1} \sum_{i=0}^K \frac{p_{ii}}{\sum_{j=0}^K p_{ij} + \sum_{j=0}^K p_{ji} - p_{ii}} \quad (3)$$

For 3D instance segmentation, Average Precision (AP) and mean class Average Precision (mAP) are also frequently used. Assuming $L_I, I \in [0, K]$ instance in every class, and c_{ij} is the amount of point of instance i inferred to belong to instance j ($i = j$ represents correct and $i \neq j$ represents incorrect segmentations).

Average Precision: is another simple metric for segmentation that computes the ratio between true positives and the total number of positive samples.

$$AP = \sum_{I=0}^K \sum_{i=0}^{L_I} \frac{c_{ii}}{c_{ii} + \sum_{j=0}^{L_I} c_{ij}} \quad (4)$$

Mean Average precision: is an extension of AP which computes per-class AP and then averages over the total number of classes K .

$$mAP = \frac{1}{K+1} \sum_{I=0}^K \sum_{i=0}^{L_I} \frac{c_{ii}}{c_{ii} + \sum_{j=0}^{L_I} c_{ij}} \quad (5)$$

For 3D part segmentation, the overall average category Intersection over Union ($mIoU_{cat}$) and overall average instance Intersection over Union ($mIoU_{ins}$) are most frequently

Table 1

Summary of popular 3D segmentation datasets, including the sensor, type, size, object class, number of classes (shown in brackets), and annotation method. “S” means synthetic environment, while “R” means real-world environment. Similarly, the symbols “Kf”, “s,” and “Mp” stands for thousand frames, can and million points. The symbol ‘–’ means information is unavailable.

Datasets	Sensors	Type	Size	Scene class (number)	Annotation method
Datasets for 3D semantic segmentation					
NYUv1 [155]	Microsoft Kinect v1	R	2347f	bedroom, cafe, kitchen, etc. (7)	Condition Random Field model
NYUv2 [156]	Microsoft Kinect v1	R	1449f	bedroom, cafe, kitchen, etc. (26)	2D annotation from AMK
SUN RGB-D [158]	Xtion LIVE PRO, MKv1/2	R	10355f	objects, room layouts, etc.(47)	2D/3D polygons+3D Bbox
SceneNN [62]	Asus Xtion PRO, MK v2	R	100s	bedroom, office, apartment, etc.(-)	3D Labels project to 2D frames
RueMonge2014 [146]	–	R	428s	window, wall, balcony, door, etc(7)	Multi-view semantic label.+CRF
ScanNet [21]	Occipital structure sensor	R	2.5Mf	office, apartment, bathroom, etc(19)	3D labels project to 2D frames
S3DIS [2]	Matterport camera	R	70496f	conference rooms, offices, etc(11)	Hierarchical labeling
Semantic3D [46]	Terrestrial laser scanner	R	1660Mp	farms, town hall, sports fields, etc (8)	Three baseline methods
NPM3D [148]	Velodyne HDL-32E LiDAR	R	143.1Mp	ground, vehicle, hunman, etc (50)	Human labeling
SemanticKITTI [5]	Velodyne HDL-64E	R	43Ks	ground, vehicle, hunman, etc(28)	Multi-scans semantic labelling
Matterport3D [12]	Matterport camera	R	194.4Kf	various rooms (90)	Hierarchical labeling
HoME [10]	Planner5D platform	S	45622f	rooms, object and etc.(84)	SSCNet+short text description
House3D [197]	Planner5D platform	S	45622f	rooms, object and etc.(84)	SSCNet+3 ways
Datasets for 3D instance segmentation					
ScanNet [21]	Occipital structure sensor	R	2.5Mf	office, apartment, bathroom, etc(19)	3D labels project to 2D frames
S3DIS [2]	Matterport camera	R	70496f	conference rooms, offices, etc(11)	Active learning method
Datasets for 3D part segmentation					
ShapeNet [217]	–	S	31963s	transportation, tool, etc.(16)	Propagat. human label to shapes
PSB [14]	Amazon’s Mechanical Turk	S	380s	human,cup, glasses airplane,etc(19)	Interactive segmentation tool
COSEG [182]	–	S	1090s	vase, lamp, guiter, etc (11)	semi-supervised learning

used. For the sake of explanation, we assume $M_J, J \in [0, L_I]$ parts in every instance, and p_{ij} as the total number of points in part i inferred to belong to part j .

Overall average category Intersection over Union: is an evaluation metric for part segmentation that measures the mean IoU averaged across K classes.

$$mIoU_{cat} = \frac{1}{K+1} \sum_{I=0}^K \sum_{J=0}^{L_I} \sum_{i=0}^{M_J} \frac{p_{ii}}{\sum_{j=0}^{M_J} p_{ij} + \sum_{i=0}^{M_J} p_{ji} - p_{ii}} \quad (6)$$

Overall average instance Intersection over Union: for part segmentation measures the mean IoU across all instances.

$$mIoU_{ins} = \frac{1}{\sum_{I=0}^K L_I + 1} \sum_{I=0}^K \sum_{J=0}^{L_I} \sum_{i=0}^{M_J} \frac{p_{ii}}{\sum_{j=0}^{M_J} p_{ij} + \sum_{i=0}^{M_J} p_{ji} - p_{ii}} \quad (7)$$

3. 3D Semantic Segmentation

Many deep learning methods for 3D semantic segmentation have been proposed in the literature. These methods can be divided into five categories according to the data representation used, namely, RGB-D image-based, projected images-based, voxel-based, point-based, 3D video,

and other representations-based. Based on the network architecture, point-based methods can be further categorized into multiple-layer perceptron (MLP) based, point convolution based, graph convolution based and point transformer based methods. Figure 5 shows the milestones of deep learning on 3D semantic segmentation in recent years.

3.1. RGB-D Based Segmentation

The depth map in an RGB-D image contains geometric information about the real world, which helps distinguish foreground objects from the background, providing opportunities to improve segmentation accuracy. In this category, the classical two-channel network is generally employed to separately extract features from both RGB and depth images. However, this straightforward framework often lacks the capacity to capture detailed and comprehensive features. To address this limitation, researchers have incorporated various additional modules into this basic two-channel framework to enhance its performance by learning more complex contextual and geometric information for segmentation accuracy. These modules can generally be categorized into six groups: multi-task learning, depth encoding, multi-scale networks, novel neural network architectures, data/feature/score level fusion and post-processing techniques (see Figure 6). Table 2 summarizes the semantic segmentation methods based on RGB-D images.

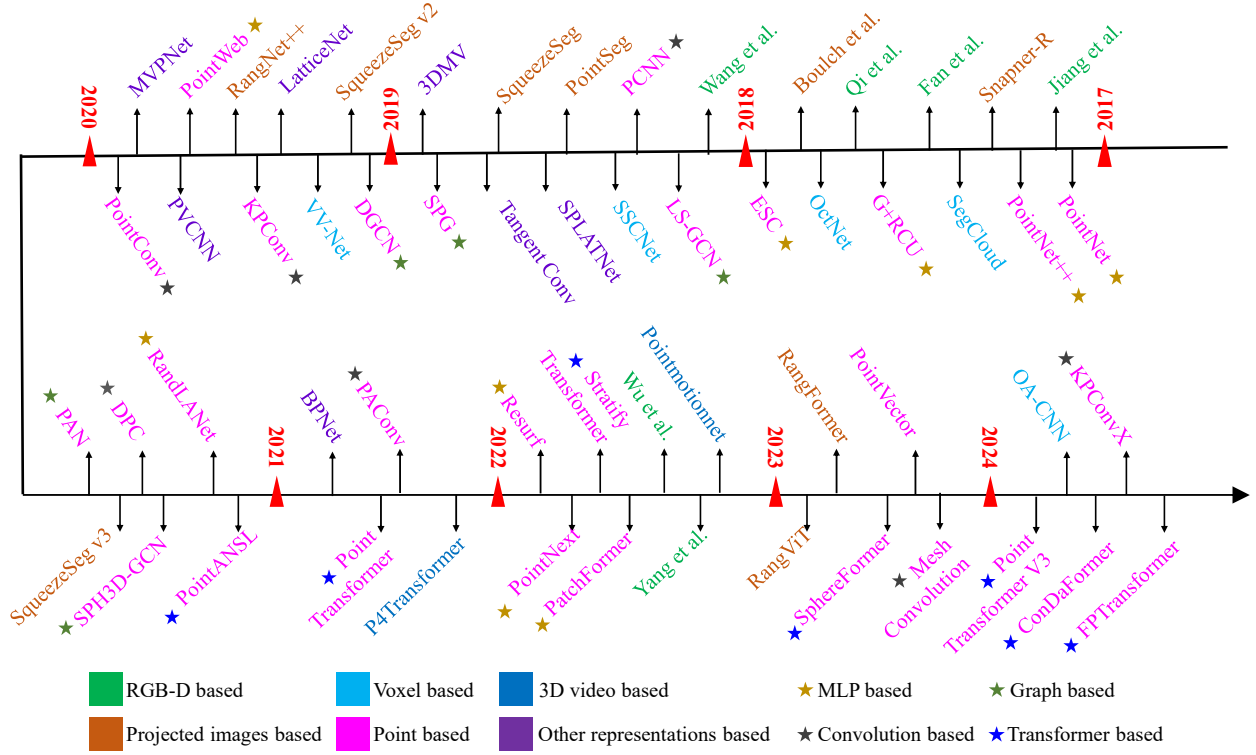


Fig. 5: Milestones of deep learning based 3D semantic segmentation methods. Note that the arrow (timeline) goes anti-clockwise

Multi-tasks learning: Depth estimation and semantic segmentation are both complex and challenging tasks in computer vision. These tasks are interrelated because the depth changes within a single object are generally smaller than the depth changes between different objects. Therefore, many researchers combine depth estimation with semantic segmentation. Based on the relationship between these two tasks, there are primarily two types of multi-task learning frameworks: cascade and parallel.

In the cascade framework, the depth estimation task first produces depth images, which are then used by the semantic segmentation task. For example, Cao et al. [11] applied deep convolutional neural fields, as introduced in [110], to estimate depth. The resulting depth and RGB images are then input into a two-channel FCN for semantic segmentation. Similarly, Guo et al. [43] used the deep network developed by Ivaneky [68] to automatically generate depth images from a single RGB image and subsequently proposed a two-channel FCN model that utilizes the RGB image and the predicted depth map for pixel-level labeling.

The cascade framework handles depth estimation and semantic segmentation separately, preventing simultaneous end-to-end training for both tasks. As a result, the semantic segmentation task does not contribute to improving the depth estimation task. On the other hand, the parallel framework integrates both tasks within a unified network, allowing them to mutually enhance each other. For example, Wang et al. [176] employed a Joint Global CNN to leverage pixel-level depth values and semantic labels from RGB images, providing accurate global scale and semantic guidance. They

also used a Joint Region CNN to extract region-level depth values and semantic maps from RGB images, enabling the learning of fine-grained depth and semantic boundaries. A multi-scale FCN [126] consists of five streams that capture depth and semantic features at various scales, where both tasks share the underlying feature representations. Liu et al. [112] proposed a collaborative deconvolutional neural network to jointly model these two tasks. However, the depth maps estimated from RGB images tend to be of lower quality compared to those obtained directly from depth sensors. As a result, this multi-task learning approach has gradually fallen out of favor in RGB-D semantic segmentation.

Depth Encoding: Traditional 2D CNNs cannot effectively capture the rich geometric features from raw depth images. An alternative approach is to transform raw depth images into representations better suited for 2D CNNs. Hoft et al. [57] used a simplified version of the histogram of oriented gradients to represent the depth channels from RGB-D scenes. Gupta et al. [45] and Aman et al. [107] derived three new channels from the raw depth images, including horizontal disparity, height above ground, and angle with gravity (HHA). Liu et al. [111] identified a limitation of HHA, noting that some scenes may lack sufficient horizontal and vertical planes. To address this problem, they propose a novel gravity direction detection method using vertical lines to improve representation learning. Hazirbas et al. [49] also argued that the HHA representation has a high computational cost and contains less information than raw depth images. They introduced an architecture called FuseNet,

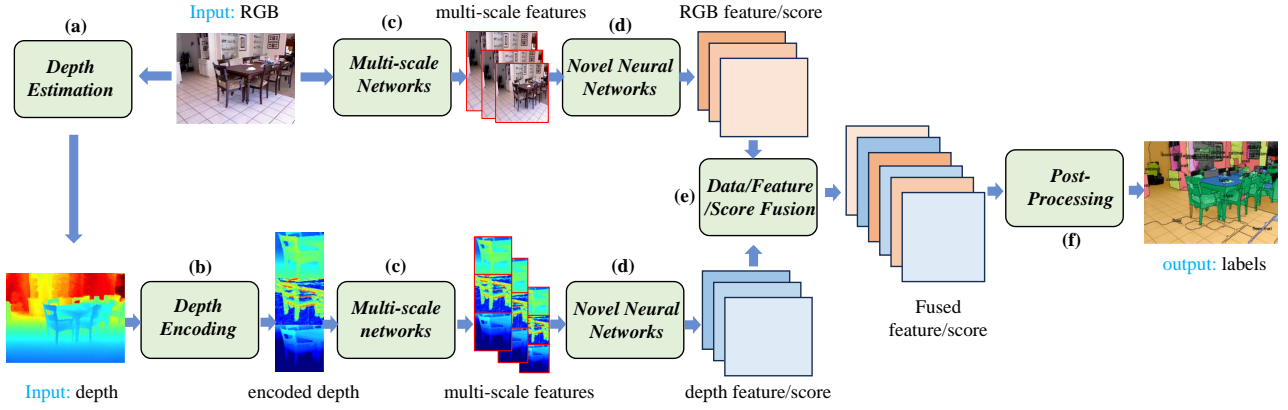


Fig. 6: Typical two-channel framework with six improvement modules, including (a) multi-task learning, (b) depth encoding, (c) multi-scale network, (d) novel neural network architecture, (e) feature/score level fusion, and (f) post-processing

which has two encoder-decoder branches—a depth branch and an RGB branch—that directly encode depth information while reducing computational complexity.

Multi-scale Network: The contextual information learned by multi-scale networks is particularly beneficial for segmenting small objects and detailed regions. To directly extract features from both RGB and depth images, Couprie et al. [20] used a multi-scale convolutional network. Similarly, Aman et al. [141] developed a multi-scale deep ConvNet for segmentation, where the coarse predictions from the VGG16-FC network are upsampled in a Scale-2 module and concatenated with the low-level predictions from the VGG-M network in a Scale-1 module, capturing both high-level and low-level features. However, this approach is sensitive to clutter in the scene, leading to output errors. Lin et al. [107] addressed this by focusing on low-resolution regions with higher depth and high-resolution regions with lower depth. They use depth maps to divide the corresponding color images into multiple scene-resolution regions and introduce a context-aware receptive field (CaRF) to concentrate on the semantic segmentation of specific scene-resolution regions, making their approach a multi-scale network.

Novel Neural Networks: Given the fixed grid computation of CNNs, their ability to process and exploit geometric information is limited. Therefore, researchers have proposed other novel neural network architectures to exploit better geometric features and the relationships between RGB and depth images. These architectures can be divided into five main categories.

- *Improved 2D Convolutional Neural Networks (2D CNNs).* Inspired by cascaded feature networks [107], the Dense-Sensitive Fully Convolutional Neural Network (DFCN) [74] integrates depth information into the early layers of the network using feature fusion techniques, followed by several dilated convolutional layers to capture contextual information. Similarly, the depth-aware 2D CNN [179] introduced a depth-aware convolution layer and a depth-aware pooling

layer, designed with the concept that pixels sharing the same semantic label and similar depth should exert a stronger influence on each other.

- *Deconvolutional Neural Networks (DeconvNets).* They provide a simple, yet effective and efficient solution for refining the segmentation map. Liu et al. [112] and Wang et al. [174] use the DeconvNet due to its strong performance. However, the potential of DeconvNets is limited as the high-level prediction map mainly gathers large-scale contexts for dense prediction. To address this problem, the Locality-Sensitive DeconvNet (LS-DeconvNet) [16] refines boundary segmentation over both depth and color images. LS-DeconvNet integrates local visual and geometric cues from the raw RGB-D data into each DeconvNet, allowing it to upsample coarse convolutional maps with extensive contexts while preserving accuracy object boundaries.
- *Recurrent Neural Networks (RNNs)* can capture long-range dependencies between pixels but are primarily designed for a single data channel, such as RGB. Fan et al. [32] extended traditional RNNs to support multiple modalities, creating multimodal RNNs (MM-RNNs) for applications like RGB-D scene labeling. MM-RNNs enable the 'memory' to be shared across both color and depth channels, allowing each channel to incorporate features and attributes from the others, thereby enhancing the discriminative power of the learned features for semantic segmentation. Additionally, a novel Long Short-Term Memorized Context Fusion (LSTM-CF) model [103] is introduced to effectively capture and integrate contextual information from multiple RGB and depth image channels.
- *Graph Neural Networks (GNNs)* are first applied to RGB-D semantic segmentation by Qi et al. [138], who projected the 2D RGB pixels into a 3D space using depth information and linked the 3D points with their corresponding semantic data. They then constructed a graph using the k-nearest neighbors of these 3D points

Table 2

The summary of RGB-D based methods with deep learning. Est. ← depth estimation. Enc. ← depth encoding. Mul. ← multi-scale networks. Nov. ← novel neural networks. Fus. ← data/feature/score fusion. Pos. ← post-processing. 2S ← 2-stream.

Methods	Est.	Enc.	Mul.	Nov.	Fus.	Pos.	Archi. (2S)	Contribution
Cao et al. [11]	✓	✓	×	×	✓	×	FCNs	Estimating depth images+a unified network for two tasks
Guo et al. [43]	✓	×	×	×	✓	×	FCNs	Incorporating depth & gradient for depth estim.
Wang et al. [176]	✓	×	×	×	×	✓	Region./Global CNN	HCRF for fusion and refining + two tasks by a network
Mousavian et al. [126]	✓	×	✓	×	✓	✓	FCN	FC-CRF for refining + Mutual improvement for two tasks
Liu et al. [112]	✓	×	×	✓	×	✓	S/D-DCNN	PBL for two feature maps integration + FC-CRF
Hofit et al. [57]	×	✓	×	×	×	×	CNNs	A embedding for depth images
Gupta et al. [45]	×	✓	×	×	×	×	CNNs	HHA for depth images
Liu et al. [111]	×	✓	×	×	✓	✓	DCNNs	New depth encoding+ FC-CRF for refining
Hazirbas et al. [49]	×	✓	×	×	✓	×	Encoder-decoder	Semantic and depth feature fusion at each layer
Coupri et al. [20]	×	×	✓	×	✓	×	ConvNets	RGB laplacian pyramid for multi-scale features
Raj et al. [141]	×	✓	✓	×	✓	×	VGG-M	New multi-scale deep CNN
Lin et al. [107]	×	×	✓	✓	✓	×	CFN	CaRF for multi-resolution features
Jiang et al. [74]	×	×	×	✓	✓	✓	RGB-FCN	Semantic & depth feature fusion at each layer + DCRF
Wang et al. [179]	×	×	×	✓	×	×	Depth-aware CNN	Depth-aware Conv. and depth aware average pooling
Cheng et al. [16]	×	✓	×	✓	✓	×	FCN + Deconv	LS-DeconvNet + novel gated fusion
Fan et al. [32]	×	×	×	✓	✓	×	MM-RNNs	Multimodal RNN
Li et al. [103]	×	✓	×	✓	✓	×	LSTM-CF	LSTM-CF for capturing and fusing contextual inf.
Qi et al. [138]	×	×	×	✓	×	×	3DGNN	GNN for RGB-D semantic segmentation
Wang et al. [174]	×	×	×	✓	✓	×	ConvNet-DeconvNet	MK-MMD for assessing the similarity between common features
Ying et al. [220]	×	×	×	✓	✓	×	Swin-Transformer	Effective and scalable fusion module based on across-attention
Wu et al. [199]	×	×	×	✓	✓	×	Swin-Transformers	Transformer-based fusion module
Yang et al. [214]	×	×	×	✓	×	×	SwinT+ResNet	Swin-RGB-D Transformer

and employed a 3D Graph Neural Network (3DGNN) to make predictions for each pixel.

- *Transformers* gained popularity in RGB image segmentation and have been extended to RGB-D segmentation. Researchers have proposed various approaches to leveraging transformers for this purpose. One notable work [220] introduces the concept of uncertainty-aware self-attention, which explicitly manages the information flow from unreliable depth pixels to confident depth pixels during feature extraction. This approach addresses the challenges posed by noisy or uncertain depth information in RGB-D segmentation. Another study [199] adopts the Swin-Transformer directly to exploit RGB and depth features. By leveraging the self-attention mechanism, this approach captures long-range dependencies and enables effective fusion of RGB and depth information for segmentation. The success of the Swin-Transformer inspires a hierarchical Swin-RGBD Transformer [214], which incorporates and leverages depth information to complement and enhance the ambiguous and obscured features in RGB images. The hierarchical architecture allows for multi-scale feature learning and enables more effective RGB and depth information integration.

Fusion: Achieving an optimal combination of texture (from the RGB channels) and geometric (from the depth channel) information is crucial for precise semantic segmentation.

Three main fusion strategies exist: data-level, feature-level, and score-level fusion, corresponding to early, middle, and late fusion, respectively. A basic data-level fusion approach involves merging the RGB and depth images into a four-channel input for direct use in a CNN model [20]. However, this data-level fusion approach fails to fully utilize the strong correlations between the depth and RGB channels. In contrast, feature-level fusion captures these correlations more effectively. For instance, a memorized fusion layer [103] adaptively merges vertical depth information with RGB contexts in a data-driven way, while also allowing bidirectional propagation along the horizontal direction to maintain true 2D global contexts.

Moreover, Wang et al. [174] introduced a feature transformation network that establishes correlations between the depth and RGB channels and connects the convolutional and deconvolutional networks within a single channel. This network can identify unique features within a single channel and common features across both channels, enabling the two branches to share features and thereby enhance the representation capability of the shared information. The complex feature-level fusion models mentioned above are inserted at a specific corresponding layer between the RGB and depth channels, which makes them difficult to train and limits the fusion of other corresponding layer features. To address this, Hazirbas et al. [49] and Jiang et al. [74] perform fusion using an element-wise summation to combine features from multiple corresponding layers between the two channels. Wu et al. [199] propose a new transformer-based fusion

approach, TransD-Fusion, to more effectively capture long-range contextual information.

Score level fusion is commonly performed using the simple averaging strategy. However, the contributions of the RGB and depth models for semantic segmentation are different. A score-level fusion layer [111] with a weighted summation uses a convolution layer to learn the weights from the two channels. Similarly, a gated fusion layer [16] learns the varying performance of RGB and depth channels for different class recognition in various scenes. Both techniques improved the results over the simple averaging strategy at the cost of additional learnable parameters.

Post-Processing: The results of CNN or DCNN used for RGB-D semantic segmentation are generally very coarse, resulting in rough boundaries and the disappearance of small objects. A standard method to address this problem is to couple the CNN with a conditional random field (CRF). The joint inference of hierarchical CRF (HCRF) [176] further boosts the mutual interactions between the two channels. It enforces synergy between global and local predictions, where the global layouts guide the local predictions and reduce local ambiguities, and local results provide detailed regional structures and boundaries. A fully connected CRF (FC-CRF) for post-processing is adopted by [126], [112], and [111], where the pixel-wise label prediction jointly considers geometric constraints, such as pixel-wise normal information, pixel position, intensity, and depth, to promote the consistency of pixel-wise labeling. Similarly, dense-sensitive CRF (DCRF) [74] integrates the depth information with FC-CRF.

3.2. Projected Images Based Segmentation

The main idea behind projected image-based semantic segmentation is to leverage 2D CNNs to extract features from 2D projections of 3D scenes or shapes and subsequently combine these features for label prediction. This approach allows for capturing richer semantic information from large-scale scenes compared to single-view images, and reduces the data size of a 3D scene relative to a point cloud. The projected images are typically multi-view or spherical images.

Among these, multi-view image projection is usually employed on RGB-D datasets [21] and statics terrestrial scanning datasets [46]. Spherical image projection is generally utilized on self-driving mobile laser scanning datasets [5]. Table 3 summarizes projected images-based semantic segmentation methods.

Multi-view image segmentation: MVCNN [161] employs a unified network to merge features from multiple views of a 3D shape captured by a virtual camera into a single, compact shape descriptor to enhance classification performance. This motivated researchers to apply a similar approach to 3D semantic segmentation (see Figure 7). For instance, Lawin et al. [90] project point clouds into multi-view synthetic images, such as RGB, depth, and surface normal images. The prediction scores from all multi-view images are fused

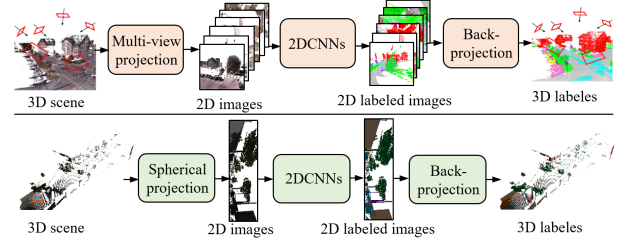


Fig. 7: Illustration of basic frameworks for projected images based segmentation methods. **Top:** Multi-view images based framework. **Bottom:** Spherical images based framework.

into a unified representation and then reprojected onto each point. However, if the point cloud is sparsely populated, the snapshot may incorrectly capture points located behind the observed structure, leading the deep network to misinterpret the various views.

To this end, SnapNet [9], [8] preprocesses point clouds by calculating point features and creating a mesh, similar to the process of point cloud densification. From the mesh and point clouds, the authors generate RGB and depth images using appropriate snapshots. They then perform pixel-wise labeling of these 2D snapshots using FCNs and rapidly reproject the labels back onto the 3D points using efficient buffering. These methods require acquiring the entire point cloud of the 3D scene beforehand to provide a complete spatial structure necessary for accurate back-projection. However, multi-view images captured directly from real-world scenes often lose significant spatial information. Some approaches attempt to combine 3D scene reconstruction with semantic segmentation, where scene reconstruction can compensate for the missing spatial data. For instance, Guerry et al. [42] reconstruct 3D scenes using global multi-view RGB and gray scale stereo images, then reproject the labels from 2D snapshots onto the reconstructed scene. However, simple back-projection does not effectively integrate semantic and spatial geometric features. In response, Pham et al. [133] proposed a novel higher-order CRF, applied after back-projection, to further refine the initial segmentation.

Spherical image segmentation:

Selecting snapshots from a 3D scene is challenging. It requires careful consideration of factors such as the number of viewpoints, the viewing distance, and the angle of the virtual cameras to optimally represent the entire scene. To bypass these complexities, researchers have projected the entire point cloud onto a sphere (see the last row of Figure 7). For example, SqueezeSeg [190], an end-to-end pipeline inspired by SqueezeNet [66], extracts features from spherical images, which are then refined by a CRF implemented as a recurrent layer. Similarly, PointSeg [183] builds on SqueezeNet by incorporating feature-wise and channel-wise attention to learn a more robust representation. SqueezeSegv2 [191] enhances SqueezeSeg's architecture with a context aggregation module, adding a LiDAR mask as an additional channel to improve noise robustness. RangeNet++ [124] transfers semantic labels back to the 3D point clouds, ensuring that no

Table 3

Summary of projected images, voxel, and other-representation based methods with deep learning. M←multi-view image. S←spherical image. V←voxel. T←tangent images. L←lattice. P←point clouds.

	Methods	Input	Architecture	Feature extractor	Contribution
projection	Lawin et al. [90]	M	multi-stream	VGG-16	Investigate the impact of different input modalities
	Boulch et al. [9] [8]	M	SegNet/U-Net	VGG-16	New and efficient framework SnapNet
	Guerry et al. [42]	M	SegNet/U-Net	VGG-16	Improved MVCNN+3D consistent data augment.
	Pham et al. [133]	M	Two-stream	2DConv	High-order CRF+ real-time reconstruction pipeline
	Wu et al. [190]	S	AlexNet	Firemodules	End-to-end pipeline SqueezeSeg + real time
	Wang et al. [183]	S	AlexNet	Firemodules	Quite light-weight framework PointSeg + real time
	Wu et al. [191]	S	AlexNet	Firemodules	Robust framework SqueezeSegV2
	Milioto et al. [124]	S	DarkNet	Residual block	GPU-accelerated post-processing + RangNet++
	Xu et al. [206]	S	RangeNet	SAC	Adopting different filters for different locations
	Ando et al. [1]	S	U-Net	ViTs	Decreasing the gaps between image and point domain.
	Kong et al. [84]	S	U-Net	ViTs	Introducing a scalable training from range view strategy
voxel	Huang et al. [64]	V	3D CNN	3DConv	Efficiently handling large data
	Tchapmi et al. [165]	V	3D FCNN	3DConv	Combining 3D FCNN with fine-represen.
	Meng et al. [122]	V	VAE	RBF	A novel voxel-based representation + RBF
	Liu et al. [109]	V	3D CNN/DQN/RNN	3DConv	Integrating three vision tasks into one frame.
	Rethage et al. [144]	V	3D FCNN	FPCov	First fully-convolutional network on raw point sets
	Dai et al. [23]	V	3D FCNN	3DConv	Combining scene completion and semantic labeling
	Riegler et al. [145]	V	Octree	3DConv	Making DL with high-resolution voxels
	Graham et al. [40]	V	FCN/U-Net	SSConv	SSConv with less computation
	Peng et al. [132]	V	U-Net	SSConv	Adaptive receptive field and adaptive relation learning
others	TangentConv [164]	T	U-Net	TConv	Tangent convolution + Parsing large scenes
	SPLATNet [160]	L	DeepLab	BConv	Hierarchical and spatially-aware feature learning
	LatticeNet [147]	L	U-Net	PN+3DConv	Hybrid architecture + novel slicing operator
	3DMV [22]	M+V	Cascade frame.	ENet+3DConv	Inferring 3D semantics from both 3D and 2D input
	Hung et al. [17]	V+M+P	Parallel frame.	SSCNet/DeepLab/PN	Leveraging 2D and 3D features
	PVCNN [115]	V+P	PointNet	PVConv	Both memory and computation efficient
	MVPNet [70]	M+P	Cascade frame.	U-Net+PointNet++	Leveraging 2D and 3D features
	LaserNet++ [123]	M+P	Cascade frame.	ResNet+LNet	Unified network for two tasks
	BPNet [61]	M+P	Cascade frame.	2/3DUNet	Bidirection projection module

points are lost regardless of the level of CNN discretization. Despite the similarities between regular RGB and LiDAR images, the feature distribution of LiDAR images varies depending on their location. SqueezeSegv3 [206] introduces a spatially-adaptive and context-aware convolution, known as spatially-adaptive convolution (SAC), which applies different filters to different locations. Inspired by the success of the 2D vision Transformer, RangViT [1] utilizes Vision Transformers (ViTs) pre-trained on extensive natural image datasets by adding downsampling and upsampling modules to the top and bottom of the ViTs, achieving superior performance compared to projection-based methods. Similarly, RangeFormer [84] uses a scalable training strategy that divides the entire projection image into several sub-images, processes them through ViTs during training, and then sequentially merges the predictions to reconstruct the full scene.

3.3. Voxel-Based Segmentation

Similar to pixels, voxels divide the 3D space into many volumetric grids with a specific size and discrete coordinates. It contains more geometric information about the scene compared to projected images. 3D ShapeNets [198]

and VoxNet [121] take volumetric occupancy grid representation as input to a 3D convolutional neural network for object recognition, which guides 3D semantic segmentation based on voxels. Voxel-based semantic segmentation methods are summarized in Table 3.

3D CNN is a typical architecture that processes uniform voxels for label prediction. 3D FCN [64] is for coarse voxel-level predictions but is limited by the spatial inconsistency between predictions and provides coarse labeling. SEGCloud [165], a novel network, produces fine-grained predictions, upsampling the coarse voxel-wise prediction obtained from a 3D FCN to the original 3D point space resolution by trilinear interpolation.

With fixed-resolution voxels, the computational complexity grows linearly with the increase in scene scale. Large voxels can lower the computational cost of large-scale scene parsing. Liu et al. [109] introduced a novel network called 3D CNN-DQN-RNN. Like the sliding windows in 2D semantic segmentation, 3D CNN-DQN-RNN proposes an eye window that traverses the whole data for fast localizing and segmenting class objects under the control of a 3D CNN and a deep Q-Network (DQN). The 3D CNN and residual RNN further refine features in the eye window.

The pipeline learns key features of interesting regions efficiently to enhance the accuracy of large-scale scene parsing with less computational cost. Rethage et al. [144] present a novel fully convolutional point network (FCPN), sensitive to multi-scale input, to parse large-scale scenes without pre- or post-process steps. Mainly, FCPN is able to learn memory-efficient representations that scale well to larger volumes.

Similarly, Dai et al. [23] design a novel 3D CNN to train on-scene subvolumes but deploy on arbitrarily large scenes at test time, as it can handle large scenes with varying spatial extent. Additionally, their network adopts a coarse-to-fine tactic to predict multiple resolution scenes to handle the resolution growth in data size as the scene increases. Traditionally, the voxel representation only comprises boolean occupancy information, which loses many geometric details. Meng et al. [122] develop a novel information-rich voxel representation by using a variational auto-encoder (VAE) and a radial basis function (RBF) to capture the distribution of points within each voxel. Further, they proposed a group equivariant convolution to exploit this feature.

In fixed-scale scenes, the computational complexity grows cubically as the voxel resolution increases. However, the volumetric representation is naturally sparse, resulting in unnecessary computations when applying 3D dense convolution to the sparse data. To address this problem, OctNet [145] divides the space hierarchically into nonuniform voxels using a series of unbalanced octrees. The tree structure allows memory allocation and computation to focus on relevant dense voxels without sacrificing resolution. However, empty space still imposes a computational and memory burden on OctNet. In contrast, Graham et al. [40] proposed a novel submanifold sparse convolution (SSC) that does not perform computations in empty regions, making up for the drawback of OctNet. OA-CNN [132] introduces adaptive receptive fields and adaptive relation into the Sparse CNN, to learn long-scale context information.

3.4. Point-Based Segmentation

Point clouds are scattered irregularly in 3D space, lacking any canonical order and translation invariance, which restricts the use of conventional 2D/3D convolutional neural networks. Recently, a series of point-based semantic segmentation networks have been proposed. These methods can be roughly subdivided into four categories: MLP-based, point convolution-based, graph convolution-based, and transformer-based. These methods are summarized in Table 4.

MLP segmentation techniques: techniques apply a MLP directly to the points to learn features. The PointNet [136] is a pioneering work that directly processes point clouds. It uses shared MLP to exploit pointwise features and adopts a symmetric function such as max-pooling to collect these features into a global feature representation. Because the max-pooling layer only captures the maximum activation across global points, PointNet cannot learn to exploit local features. Building on PointNet, PointNet++ [137] defines a hierarchical learning architecture. It hierarchically samples

points using farthest point sampling (FPS) and groups local regions using k nearest neighbor search and ball search. Progressively, a simplified PointNet exploits features in local regions at multiple scales or resolutions. Similarly, Engelmann et al. [31] define local regions by KNN and K-means clustering and use a simplified PointNet to extract local features.

To learn the short- and long-range dependencies, some works introduce RNNs to MLP-based methods. For example, ESC [29] divides global points into multi-scale/grid blocks. The concatenated (local) block features are appended to the pointwise features and passed through Recurrent Consolidation Units (RCUs) to further learn global context features. Similarly, HRNN [215] uses pointwise pyramid pooling (3P) to extract local features from multi-size local regions. Pointwise features and local features are concatenated, and a two-direction hierarchical RNN explores context features on these concatenated features. However, the local features learned are insufficient because the deeper layer features do not cover a larger spatial extent.

Some works integrate the hand-crafted point representation into the PointNet or PointNet++ network to enhance the point representation ability with less learnable network parameters. Inspired by SIFT representation [116], PointSIFT [76] inserts a PointSIFT module layer to learn local shape information. This module transforms each point into a new shape representation by encoding information about different orientations. PointWeb [228] proposes an adaptive feature adjustment (AFA) module to learn the interactive information between local points to enhance the point representation. Similarly, RepSurf [142] introduces two novel point representations, namely triangular and umbrella representative surfaces, to establish connections and enhance the representation capability of learned point-wise features.

This approach effectively improves feature representation with fewer learnable network parameters, drawing significant attention from the research community. In contrast to the aforementioned methods, PointNeXt [139] takes a different approach by revisiting the classical PointNet++ architecture through a systematic study of model training and scaling strategies. It proposes improved training strategies that lead to a significant performance boost for PointNet++. Additionally, PointNeXt introduces an inverted residual bottleneck design and employs separable MLPs to enable efficient and effective model scaling. Similarly, PointVector [24] proposes a Vector-oriented point set abstraction that can aggregate neighboring features through high-dimensional vectors.

Point convolution techniques: perform convolution operations directly on the points. Different from 2D convolution, the weight function of a point convolution needs to be learned from point geometric information adaptively. Early convolutional networks focused on the convolution weight function design. For example, RSNet [65] exploits point-wise features using 1×1 convolution and then passes them through the local dependency module (LDM) to exploit

Table 4

Summary of point based semantic segmentation methods with deep learning. Here, ‘Nb’ stands for Neighbour, ‘part.’ is for partition.

	Methods	Nb. Search	Feature abstraction	Coarsening	Contribution
MLP	PointNet [136]	None	MLP	None	Pioneering processing points directly
	G+RCU [31]	None	MLP	None	Two local definition+local/global pathway
	ESC [29]	None	MLP	None	MC/Grid Block for local defini.+RCUs for context
	HRNN [215]	None	MLP	None	3P for local feature +HRNN for local context
	PointNet++ [137]	Ball/KNN	PointNet	FPS	Proposing hierarchical learning framework
	PointSIFT [76]	KNN	PointNet	FPS	PointSIFT module for local shape information
	PointWeb [228]	KNN	PointNet	FPS	AFA for interactive feature exploitation
	Repsurf [142]	KNN	PointNet	FPS	Local triangular orient. + local umbrella orient.
	PointNeXt [139]	KNN	InvResMLP	FPS	Next version of PointNet
	PointVector [24]	KNN	PointNet	FPS	A vector oriented point set abstraction
Point Convolution	RSNet [65]	None	1x1 Conv	None	LDM for local context exploitation
	DPC [30]	DKNN	PointConv	None	Dilated KNN for expanding the receptive field
	PointWiseCNN [63]	Grid	PWConv.	None	Novel point convolution
	PCCN [178]	KD index	PCCConv.	None	KD-tree index for neigh. search+novel point Conv.
	KPConv [166]	Ball	KPConv.	Grid Samp.	Novel point convolution
	KPConvX [24]	Ball	KPConvX	Grid Samp.	Novel Point Convolution
	FlexConv [41]	KD index	flexConv.	IDISS	Novel point Conv.+flex-maxpooling no subsampling
	PointCNN [101]	DKNN	χ -Conv	FPS	Novel point convolution
	MCC [56]	Ball	MCCConv.	PDS	Novel coarsening layer+point convolution
	PointConv [193]	KNN	PointConv	FPS	Novel point convolution considering point density
	A-CNN [83]	DKNN	AConv	FPS	Novel neighborhood search+point convolution
	RandLA-Net [60]	KNN	LocSE	RPS	LFAM with large receptive field & geometric details
	PolarNet [226]	None	PointNet	PolarGrid	Novel local regions definition + RingConv
Graph Convolution	DGCNN [184]	KNN	EdgeConv	None	Novel graph convolution + updating graph
	SPG [89]	partition	PointNet	None	Superpoint graph + parsing large-scale scene
	DeepGCNs [96]	DKNN	DGConv	RPS	Adapting residual connections between layers
	SPH3D-GCN [94]	Ball	SPH3D-GConv	FPS	Novel graph convolution + pooling + uppooling
	LS-GCN [171]	KNN	Spec.Conv.	FPS	Local spectral graph + Novel graph convolution
	PAN [34]	Multi-direct.	LAE-Conv	PFS	Point-wise spatial attention+local graph Conv.
	TGNet [102]	Ball	TGConv	PFS	Novel graph Conv.+multi-scale features explo.
	HDGCN [105]	KNN	DGConv	FPS	Depthwise graph Conv. + Pointwise Conv.
	3DCon.Net [224]	KNN	PointNet	Tree layer	KD tree structure
	ψ -CNN [92]	Octree neig.	ψ -Conv	Tree layer	Octree structure+ Novel graph convolution
Point Transformer	PGCRNet [119]	None	Conv1D	None	PointGCR to model context dependencies
	AGCN [205]	KNN	MLP	None	Point attention layer for aggregating local features
	PointANSL [211]	KNN	local-nonlocal module	AS	Local-nonlocal module + adaptive sampling
	Point Transformer [229]	KNN	Point Transformer	Maxpooling	MLP-based relative position encoding + vec. atten.
	Point Transformer v2 [195]	Grid part.	Point Transformer v2	Gridpooling	Novel position encoding + Grid pooling
	FPTTransformer [55]	KNN	Full point transformer	SADS	Full point encoding + shape aware downsampling
	PatchFor. [225]	Boxes part.	Patch Transformer	DWConv	First linear attention + Lightweight multi-scale
	Fast Point Transfor. [130]	Voxel part.	Fast point Transformer	Voxel Samp.	Lightweight local self-attention + position encoding
	Stratified Transfor. [88]	Voxel part.	Stratified Transformer	PFS	Contextual relative position encoding
	SphereFormer [87]	Voxel part.	Spherefor. + cubicfor.	Maxpooling	Novel spherical window for LIDAR points
	ConDaFormer [25]	Voxel part.	ConDaFormer	Maxpooling	Disassembled window attention module
	Point Transformer v3 [194]	Spatial proximity	Point Transformer v3	Gridpooling	Streamlined approach tailored for serialized point clouds

local context features. However, it does not define each point’s neighborhood to learn local features. On the other hand, PointwiseCNN [63] sorts points in a specific order, e.g., XYZ coordinates or Morton curve [125], and queries nearest neighbors dynamically and bins them into 3×3×3 kernel cells before convolving with the same kernel weights.

Gradually, some point convolution methods approximate the convolution weight function as MLP to learn weights from point coordinates. PCCN [178] performs parametric

CNN, where the kernel is estimated as an MLP, on KD-tree neighborhoods to learn local features. PointCNN [101] coarsens the input points with the FPS. The convolution layer learns an χ transformation from local points by MLP to simultaneously weight and permute the features, subsequently applying a standard convolution to these transformed features.

Some work associates a coefficient (derived from point coordinates) with the weight function to adjust the learned

convolutional weights. An extension of the Monte Carlo approximation for convolution called PointConv [193] considers the point density. It uses MLP to approximate a weight function of the convolution kernel and applies an inverse density scale to reweight the learned weight function. Similarly, MCC [56] phrases convolution as a Monte Carlo integration problem by relying on the joint probability density function (PDF), where an MLP also represents the convolution kernel. Moreover, it introduces Poisson-disk sampling (PDS) [186] to construct a point hierarchy instead of FPS, which provides an opportunity to get the maximal number of samples in a receptive field.

Another line of work employs another function instead of MLP to approximate the convolution weight function. Flex-Convolution [41] uses a linear function with fewer parameters to model a convolution kernel and adapts inverse density importance sub-sampling (IDISS) to coarsen the points. KPConv [166] and KCNet [150] fixed the convolution kernel for robustness to varying point densities. These networks predefine the kernel points on the local region and learn convolutional weights on the kernel points from their geometric connections to local points using linear and Gaussian correlation functions, respectively. Furthermore, KPConvX [167] scales the depth wise convolutional weights with kernel attention values. Here, the number and position of kernel points need to be optimized for different datasets.

Point convolution on a limited local receptive field could not exploit long-range features. Therefore, some works introduce the dilated mechanism into point convolution. Dilated point convolution (DPC) [30] adapts standard point convolution to the neighborhood points of each point, where the neighborhood points are determined through a dilated KNN search. Similarly, A-CNN [83] defines a new local ring-shaped region by dilated KNN and projects points on a tangent plane to further order neighbor points in local regions. Then, the standard point convolutions are performed on these ordered neighbors, represented as a closed-loop array.

In the large-scale point cloud semantic segmentation area, RandLA-Net [60] uses random point sampling instead of the more complex point selection approach. It introduces a novel local feature aggregation module (LFAM) to increase the receptive field and effectively preserve geometric details progressively. Another technology, PolarNet [226], first partitions a large point cloud into smaller grids (local regions) along their polar bird's-eye-view (BEV) coordinates. It then abstracts local region points into a fixed-length representation using a simplified PointNet, and these representations are passed through a standard convolution.

Graph convolution methods: perform convolution on points connected with a graph structure, where the graph helps the feature aggregation exploit the structure information between points. The graphs can be divided into spectral graphs and spatial graphs. In the spectral graph, LS-GCN [171] adopts the basic architecture of PointNet++, replaces MLPs with a spectral graph convolution using standard unparameterized Fourier kernels, as well as a novel recursive spectral

cluster pooling substitute for max-pooling. However, transformation from the spatial to the spectral domain incurs a high computational cost. Besides that, spectral graph networks are usually defined on a fixed graph structure and are thus unable to process data with varying graph structures directly.

In the spatial graph category, ECC [157] is among the pioneering methods to apply spatial graph networks to extract features from point clouds. It dynamically generates edge-conditioned filters to learn edge features describing relationships between a point and its neighbors. Based on PointNet architecture, DGCNN [184] implements a dynamic edge convolution called EdgeConv in the neighborhood of each point. A simplified PointNet approximates the convolution. SPG [89] parts the point clouds into a number of simple geometrical shapes (termed super-points) and builds a super graph on global super-points. Furthermore, this network adopts PointNet to embed these points and refines the Gated Recurrent Unit (GRU) embedding. Based on the basic architecture of PointNet++, Li et al. [102] proposed Geometric Graph Convolution (TGCov), with its filters defined as products of local point-wise features with local geometric connection features expressed by Gaussian weighted Taylor kernels. Feng et al. [34] constructed a local graph on neighborhood points searched along multi-directions and explored local features by a local attention-edge convolution (LAE-Conv). These features are imported into a point-wise spatial attention module to capture accurate and robust local geometric details. Lei et al. [93] design a fuzzy coefficient to times weight function to enable the convolution weights to be robust.

Continuous graph convolution also incurs a high computational cost and generally suffers from the vanishing gradient problem. Inspired by the separable convolution strategy in Xception [18] that significantly reduces parameters and computation burden, HDGCN [105] designed a DGConv that composes depth-wise graph convolution followed by a point-wise convolution and adds DGConv to the hierarchical structure to extract local and global features. DeepGCNs [96] borrow some concepts from 2D CNN, such as residual connections between different layers (ResNet), to alleviate the vanishing gradient problem and dilation mechanisms to allow the GCN to go deeper. The discrete spherical convolution kernel (SPH3D kernel) [94] consists of spherical convolution learning depth-wise features while point-wise convolution learning point-wise features.

Tree structures such as KD-tree and Octree can be viewed as a particular type of graph, allowing for the sharing of convolution layers depending on the tree splitting orientation. 3DContextNet [224] adopts a KD-tree structure to hierarchically represent points where the nodes of different tree layers represent local regions at various scales and employs a simplified PointNet with a gating function on nodes to explore local features. However, their performance depends heavily on the randomization of the tree construction. Lei et al. [92] built an Octree-based hierarchical structure on global points to guide the spherical convolution

computation per network layer. The spherical convolution kernel systematically partitions a 3D spherical region into multiple bins that specify learnable parameters to weight the points falling within the corresponding bin.

Transformer-based approaches: have recently become famous for improving point cloud segmentation accuracy. Compared to point convolution, the Transformer introduces point features into weight learning. For example, the authors of [119] use the channel self-attention mechanism to learn independence between any two point-wise feature channels and further define a channel graph where the channel maps are presented as nodes and the independence as graph edges. AGCN [205] integrates the attention mechanism with GCN for analyzing the relationships between local features of points and introduces a global point graph to compensate for the relative information of individual points. Likewise, PointANSL [211] utilizes the general self-attention mechanism for group feature updating and proposes an adaptive sampling (AS) module to overcome the issues of FPS.

The transformer employs self-attention as a fundamental component and includes position encoding to capture the sequential order of input tokens. Position encoding is crucial to ensure that the model understands the relative positions of tokens within a sequence. Point Transformer [229] introduces MLP-based position encoding into vector attention and uses a KNN-based downsampling module to decrease the point resolution. A follow-up work is Point Transformer v2 [195], strengthening the position encoding mechanism by applying an additional encoding multiplier to the relation vector and designing a partition-based pooling strategy to align the geometric information. FPTransformer [55] introduces the full point encoding into the local point transformer to simultaneously learn the local, global and local-global features.

Point transformers are typically computationally expensive because the original self-attention module needs to generate a considerable attention map. To address this problem, PatchFormer [225] calculates the attention map via low-rank approximation. Similarly, FastPointTransformer [130] introduces a lightweight local self-attention module that learns continuous positional information while reducing space complexity. Motivated by the success of the window-based transformer in the 2D domain, Stratified Transformer [88] designs a cubic window and samples distant points as keys, but more sparsely, to expand the receptive field. Besides, SphereFormer [87] designs radial window self-attention that partitions that space into several non-overlapping narrow and long windows for exploiting long-range dependencies. Most of transformer methods apply the transformer in a local region such as spherical or cubic window, which requires high computational cost. ConDaFormer [25] address this problem by disassembling cubic windows into orthogonal 2D planes and enhancing local structures with depth wise convolution. To balance the accuracy and efficiency, Point Transformer v3 [194] prioritizes simplicity and efficiency over the accuracy of certain mechanisms. This model replacing the precise neighbor search by KNN with an efficient

serialized neighbor mapping, which expand the receptive field from 16 to 1024 points while remaining efficient.

3.5. 3D Video Based Segmentation

Compared to the 3D single frame/scan semantic segmentation methods reviewed earlier, 3D video (continuous frames/scans) semantic segmentation methods take into account the connecting spatiotemporal information between frames, which is more effective at parsing the scene robustly and continuously. Conventional CNNs are not designed to exploit the temporal information between frames. A common strategy is to adapt recurrent neural networks or spatiotemporal convolutional networks.

RNNs: generally work in combination with 2D CNNs to process RGB-D videos. The 2D CNN extracts the frame-wise spatial information, and the RNN learns the temporal information between the frames. Valipour et al. [168] proposed a recurrent fully neural network to operate over a sliding window over the RGB-D video frames. Specifically, the convolutional gated recurrent unit preserves the spatial information and reduces the parameters. Similarly, In [27], Yurdakul et al. combine a fully convolutional and RNN to investigate the contribution of depth and temporal information separately in the synthetic RGB-D video.

Spatio-temporal convolution methods: Nearby video frames provide diverse viewpoints and additional context for objects and scenes. STD2P [54] operates a novel spatiotemporal pooling layer to aggregate region correspondences computed by optical flow and image boundary-based superpixels. Choy et al. [19] proposed 4D Spatio-Temporal ConvNet to process a 3D point cloud video directly. To overcome challenges in high-dimensional 4D space (3D space and time), they introduced the 4D spatial-temporal convolution, a generalized sparse convolution, and the trilateral-stationary conditional random field that keeps spatiotemporal consistency. Likewise, based on 3D sparse convolution, SpSequenceNet [151] contains two novel modules, a cross-frame global attention module and a cross-frame local interpolation module, to exploit spatial and temporal features in 4D point clouds. PointMotionNet [172] proposes a spatiotemporal convolution that exploits a time-invariant spatial neighboring space and extracts spatiotemporal features to distinguish between moving and static objects. TVSN [153] built a temporal graph on the 3D point cloud sequences and captures the temporal variation with a graph convolution, transforming coarse predictions into fine predictions.

Spatio-temporal transformer techniques: Point tracking is usually employed to capture the dynamics in point cloud videos. However, P4Transformer [33] offers a 4D convolution to embed the spatiotemporal local structures in point cloud video and further introduces a transformer to leverage the motion information across the entire video by performing the self-attention on these embedded local features. Also, PST² [187] performs spatiotemporal self-attention

across adjacent frames to capture the spatiotemporal context and proposes a resolution embedding module to enhance the resolution of feature maps by aggregating features. X4D-Transformer [77] leverages texture priors from RGB sequences using a dual-branch transformer into 3D point clouds sequences, to enhance 3D video understanding.

3.6. Other Representation Based Methods

Some methods transform the original point cloud into representations other than projected images, voxels, and points. Examples of such representations include tangent images [164] and lattice [160], [147]. In the former case, Tatarchenko et al. [164] project local surfaces around each point to a series of 2D tangent images and develop a tangent convolution-based U-Net to extract features. In the latter case, SPLATNet [160] adapts the bilateral convolution layers (BCLs) proposed by Jampani et al. [69] to map disordered points onto a sparse lattice smoothly. Besides, LatticeNet [147] employs a hybrid architecture that combines PointNet, which obtains low-level features, with sparse 3D convolution, which explores global context features. These features are embedded into a sparse lattice that allows the application of standard 2D convolutions.

Although the above methods have achieved significant progress in 3D semantic segmentation, each has drawbacks. For instance, multi-view images have more spectral information, like color or intensity, but fewer geometric details on the scene. On the other hand, voxels have more geometric information but less spectral information. To get the best of both worlds, some methods adopt hybrid representations as input to learn comprehensive features of a scene. Dai et al. [22] map 2D semantic features obtained by multi-view networks into 3D grids of scenes. These pipelines make 3D grids attach rich 2D semantic as well as 3D geometric information so that the scene can get better segmentation by a 3D CNN.

Likewise, Hung et al. [17] back-project 2D multi-view image features onto the 3D point cloud space and use a unified network to extract local details and global context from sub-volumes and the global scene, respectively. Liu et al. [115] argue that voxel-based and point-based NN are computationally inefficient in high-resolution and data structuring. To overcome these challenges, they propose Point-Voxel CNN (PVCNN), which represents the 3D input data as point clouds to take advantage of the sparsity to lower the memory footprint and leverage the voxel-based convolution to obtain a contiguous memory access pattern. Jaritz et al. [70] proposed MVPNet that collects 2D multi-view dense image features into 3D sparse point clouds and then uses a unified network to fuse the semantic and geometric features. Also, Meyer et al. [123] fuse 2D image and point clouds to address 3D object detection and semantic segmentation by a unifying network. BpNet [61] consists of 2D and 3D sub-networks with symmetric architectures connected through a bidirectional projection module (BPM). This allows the interaction of complementary information from both visual domains at multiple architectural levels, improving scene recognition by leveraging the advantages of

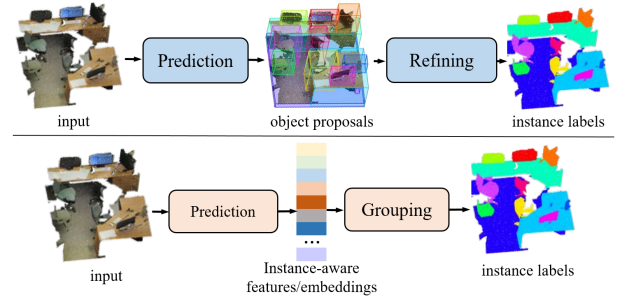


Fig. 8: Illustration of two different approaches for 3D instance segmentation. **Top row:** proposal-based framework. **Bottom row:** proposal-free framework.

both 2D and 3D information. The other representation-based semantic segmentation methods are summarized in Table 3.

4. 3D Instance Segmentation

3D instance segmentation methods additionally distinguish between different instances of the same class. Being a more informative task for scene understanding, 3D instance segmentation is receiving increased interest from the research community. 3D instance segmentation methods are roughly divided into two directions: proposal-based and proposal-free.

4.1. Proposal-Based Methods

Proposal-based methods first predict object proposals and then refine them to generate final instance masks (see Figure 8), breaking down the task into two main challenges. Hence, from the proposal generation point of view, these methods can be grouped into detection-based and detection-free methods.

Detection-based methods: often treat object proposals as a 3D bounding box regression problem. For example, 3D-SIS [58] integrates high-resolution RGB images with voxels, aligned according to the 3D reconstruction pose, and jointly learns color and geometric features using a 3D detection backbone to predict 3D bounding box proposals. In these proposals, a 3D mask backbone is used to predict the final instance masks. Similarly, GPSN [219] introduces a 3D object proposal network that reconstructs object shapes from noisy observations to improve geometric understanding. GPSN is also embedded into a 3D instance segmentation network called Region-based PointNet (R-PointNet), which refines, accepts, or rejects proposals. These networks require a step-by-step training process, and proposal refinement can be computationally expensive due to suppression operations. To overcome these challenges, 3D-BoNet [212] proposes an innovative end-to-end network that directly learns a fixed number of 3D bounding boxes without needing proposal rejection, followed by the estimation of an instance mask within each bounding box.

Detection-free methods: include SGPN [180], which assumes that points belonging to the same object instance should have similar features. It learns a similarity matrix to

Table 5

Summary of 3D instance segmentation methods with deep learning. M←multi-view image; Me←mesh; V←voxel; P←point clouds.

	Methods	Input	Propo./Embed. Prediction	Refining/Grouping	Contribution
Proposal based	GSPN [219]	P	GSPN	R-PointNet	New proposal generation methods
	3D-SIS [58]	M+V	3D-RPN+3D-RoI	3DFCN	Learning bounding box on geometry and RGB
	3D-BoNet [212]	P	Bounding box regression	Point mask prediction	Directly regressing 3D bounding box
	SGPN [180]	P	SM + SCM + PN	Non-Maximum suppre.	New group proposal
	3D-MPA [28]	P	SSCNet	Graph ConvNet	Multi proposal aggregation strategy
	AS-Net [73]	P	Four branches with MLPs	Candidate prop. suppre.	Novel Algorithm mapping labels to candidates
	SoftGroup [170]	P	Soft-grouping module	top-down refinement	Novel clustering algorithm based on dual coordinate sets
	SSTNet [104]	p	Tree traversal + splitting	CliqueNet	Constructing the superpoint tree for instance segmentation
Proposal free	3D-BEVIS [26]	M	U-Net/FCN + 3D prop.	Mean-shift clustering	Joint 2D-3D feature
	PanopticFus [127]	M	PSPNet/Mask R-CNN	FC-CRF	Coopering with semantic mapping
	ASIS [181]	P	1 encoder+ 2 decoders	ASIS module	Simultaneously performing sem./ins. segmentation tasks
	JSIS3D [134]	P	MT-PNet	MV-CRF	Simultaneously performing sem./ins. segmentation tasks
	3D-GEL [106]	P	3D U-Net	GCN	Structure-aware loss function + attention-based GCN
	OccuSeg [47]	P	3D U-Net	Graph-based clustering	Proposing a novel occupancy signal
	MASC [108]	Me	3D U-Net	Clustering algorithm	Novel clustering based on affinity and mesh topology
	MTML [86]	V	3D U-Net	Mean-shift clustering	Multi-task learning
	PointGroup [75]	P	3D U-Net	Clustering + ScoreNet	Novel clustering algorithm based on dual coordinate sets
	HAIS [13]	P	3D U-Net	Set aggregation	Hierarchical aggregation for fine-grained predictions
	Dyco3D [52]	P	3D U-Net	Dynamic conv.	Generating kernel by clustering for convolution
	PointInst3D [53]	P	3D U-Net	MLP	Generating kernel by FPS
	DKNet [196]	P	3D U-Net	MLP	Generating kernel by candidate mining and aggregation
	ISBNet [129]	P	3D U-Net	Box-aware dynamic conv	Generating kernel by instance aware FPS and point aggrega.
	Spherical Mask [154]	P	3D U-Net	Radial point migration	Radial instance detection
	SPFormer [163]	P	3D U-Net	Query Decoder	Generating instance by transformer
	Mask3D [149]	P	3D U-Net	Transformer Decoder	Generating instance by transformer
	QueryFormer [117]	P	3D U-Net	Affiliated Transformer Decoder	Generating instance by transformer
	Oneformer [82]	P	3D U-Net	Transformer Decoder	A unify network for 3D segmentation

predict proposals, and confidence scores of the points are used to prune proposals, generating highly reliable instance predictions. However, this simple distance-based similarity metric lacks informativeness and struggles to segment adjacent objects of the same class. In contrast, 3D-MPA [28] generates object proposals by learning from sampled and grouped point features that vote for the same object center, then refines the proposal features using a graph convolutional network, enabling higher-level interactions between proposals for more accurate results. AS-Net [73] employs an assignment module to allocate proposal candidates and removes redundant ones through a suppression network. SoftGroup [170] introduces top-down refinement for instance proposals. SSTNet [104] presents an end-to-end Semantic Superpoint Tree Network (SSTNet), which generates object instance proposals directly from scene points. A key innovation of SSTNet is the construction of an intermediate semantic superpoint tree (SST) based on the learned semantic features of superpoints.

4.2. Proposal Free Methods

Proposal-free methods learn feature embeddings for each point and then apply clustering to obtain definitive 3D instance labels as shown in Figure 8, breaking down the task into two main challenges. From the embedding learning point of view, these methods can be roughly subdivided into five categories: 2D embedding-based, multi-task learning,

clustering-based, dynamic convolution-based and dynamic transformer-based.

2D embedding based strategies: One example is 3D-BEVIS [26], which learns a 2D global instance embedding from a bird's-eye view of the entire scene and then propagates this embedding onto point clouds using DGCNN [184]. Another example is PanopticFusion [127], which employs the 2D instance segmentation network Mask R-CNN [51] to predict pixel-wise instance labels for RGB frames and then incorporates these predicted labels into 3D volumes.

Multi-tasks learning methods:, such as 3D semantic and 3D instance segmentation, can mutually enhance each other. For example, objects from different classes must be distinguished as separate instances, while those sharing the same instance label should belong to the same class. Building on this concept, ASIS [181] introduces an encoder-decoder network designed to learn semantic-aware instance embeddings, improving the performance of both tasks. Similarly, JSIS3D [134] utilizes a unified network, named MT-PNet, to predict semantic labels for points and embed them into high-dimensional feature vectors, while also employing MV-CRF to jointly optimize object classes and instance labels. Likewise, Liu et al. [108] and 3D-GEL [106] leverage SSCN to simultaneously produce semantic predictions and instance embeddings, with two GCNs refining the instance labels.

OccuSeg [47] applies a multi-task learning network to generate both occupancy signals and spatial embeddings, where the occupancy signal reflects the number of voxels occupied per voxel.

Clustering based techniques: like MASC [108], leverage the powerful capabilities of SSCN [40] to predict similarity embeddings between neighboring points across multiple scales and semantic structures. A straightforward yet effective clustering technique [114] is applied to segment points into instances using these two types of learned embeddings. MTML [86] employs two sets of feature embeddings: one for capturing unique instance-specific features and another for direction embedding, providing stronger cohesion for grouping. Similarly, PointGroup [75] forms clusters by combining original and shifted coordinate embedding spaces, with ScoreNet assisting in selecting optimal clusters. While these approaches group points based on point-level embeddings, they lack instance-level adjustments. HAIS [13] addresses this by introducing set aggregation and intra-instance prediction to refine object-level instances.

Dynamic convolution-based approaches: overcome the limitations of clustering-based methods by generating kernels and then convolving with the point features to generate instance masks. Dyco3D [52] adopts the clustering algorithm to generate a kernel for convolution. Similarly, PointInst3D [53] uses FPS to generate kernels. DKNNet [196] introduces candidate mining and candidate aggregation to generate more instance kernels. Moreover, ISBNNet [129] proposes a new instance encoder combining instance-aware PFS with a point aggregation layer to generate kernels to replace clustering in DyCo3D. Spherical Mask [154] uses the similar backbone as ISBNNet. It introduces spherical representation to overcome size overestimation and error propagation, significantly improving instance segmentation performance.

Dynamic transformer-based approaches: can learn more precious context information, being more conducive to identify the instances. SPFormer [163] groups potential features from point clouds into superpoint and predicts instance through query attention without relying on the results of detection and segmentation. Mask3D [149] directly predict instance mask from point clouds using instance queries, eliminating the need for traditional voting mechanisms and geometric clustering techniques. Similarly, QueryFormer [117] enhances instance segmentation by optimizing query initialization for better coverage and reducing noise through a specialized transformer decoder, resulting in more accurate instance masks and semantic labels. Oneformer [82] introduces a unified 3D segmentation framework performs 3D segmentation using a group of learnable kernels. These kernels are trained with a transformer based decoder with unified instance and semantic queries passed as an input. Table 5 summarizes 3D instance segmentation methods.

5. 3D Part Segmentation

3D part segmentation is the next finer level, after instance segmentation, where the aim is to label different parts of an instance. The pipeline of part segmentation is quite similar to semantic segmentation, except that the labels are now for individual parts. Therefore, some existing 3D semantic segmentation networks [122], [40], [136], [137], [224], [65], [166], [63], [56], [193], [101], [184], [94], [205], [178], [41], [92], [160], [147], [24], [139], [229] can also be trained for part segmentation. However, these networks can not entirely tackle the difficulties of part segmentation. For example, various parts with the same semantic label might have diverse shapes, and the number of parts for an instance with the same semantic label may be different. We subdivide 3D part segmentation methods into the following categories: regular data based and irregular data based.

5.1. Segmentation of Regular Data

Regular data usually includes projected images [78], voxels [185], [91], [159]. As for projected images, Kalogerakis et al. [78] obtain a set of images from multiple views that optimally cover the object surface and then use multi-view Fully Convolutional Networks (FCNs) and surface-based Conditional Random Fields (CRFs) to predict and refine part labels separately. Voxel is a useful representation of geometric data. However, fine-grained tasks like part segmentation require high-resolution voxels with more detailed structure information, which leads to high computation costs. VoxSegNet [185] exploits more detailed information from voxels with limited resolution. They use spatial dense extraction to preserve the spatial resolution during the sub-sampling process and an attention feature aggregation (AFA) module to adaptively select scale features. PointGrid [91] incorporates a constant number of points with each cell, allowing the network to learn better local geometry shape details. Furthermore, multiple model fusion can enhance segmentation performance. Combining the advantages of images and voxels, Song et al. [159] proposed a two-stream FCN, termed AppNet and GeoNet, to explore 2D appearance and 3D geometric features from 2D images. In particular, their VolNet extracts 3D geometric features from 3D volumes, guiding GeoNet in extracting features from a single image.

5.2. Segmentation of Irregular Data

Irregular data representations usually include meshes [207], [48] and point clouds [97], [150], [218], [169], [175], [221], [233], [223]. Mesh provides an efficient approximation to a 3D shape because it captures the flat, sharp, and intricate surface shape and topology. Xu et al. [207] put the face normal and face distance histogram as the input of a two-stream framework and use the CRF to optimize the final labels. Inspired by traditional CNN, Hanocka et al. [48] design novel mesh convolution and pooling to operate on the mesh edges.

Similar to MLP-based methods for point clouds semantic segmentation, CurveNet [200] aggregates hypothetical

Table 6

Summary of 3D part segmentation methods. M←multi-view image; Me←mesh; V←voxel; P←point clouds; reg.←regular data; irreg.←irregular data; MS.←Multi-Stream; 2S.←2-Stream.

	Methods	Input	Archi.	Backbone	Contribution
Regular	ShapeFCN [78]	M	MS-FCN	2DConv	Per-label confidence maps + surface-based CRF
	VoxSegNet [185]	V	3DU-Net	AtrousConv	SDE for preserving the spatial resolution AFA for feature selecting
	Pointgrid [91]	V	Conv-deconv	3DConv	Learning higher order local geometry shape.
	SubvolumeSup [159]	M+V	2S-FCN	2D/3DConv	GeoNet/AppNet for 3/2D features exploi. + DCT for aligning.
Irregular	DCN [207]	Me	2S-DCN & NN	DConv	DCN/NN for local feature and global feature.
	MeshCNN [48]	Me	2D CNN	MeshConv	Novel mesh convolution and pooling
	PartNet [221]	P	RNN	PN	Part feature learning scheme for context and geometry feature exploitation
	SSCNN [218]	P	FCN	SpectralConv	STN for allowing weight sharing, spectral multi-scale kernel
	CurveNet [200]	P	PN++	MLP	A hypothetical curve representation
	PointMLP [118]	P	PN++	MLP	A lightweight geometric affine module
	SPoTr [131]	P	PN++	Transformer	Self-positioning global cross-attention
	KCNet [150]	P	PN	MLP	KNN graph on points, kernel correlation for measuring geometric affinity
	SFCN [175]	P	FCN	SFConv	Novel point convolution
	SpiderCNN [209]	P	PN	SpiderConv	Novel point convolution
	FeaStNet [169]	P	U-Net	GConv	Dynamic graph convolution filters
	Kd-Net [80]	P	Kd-tree	Affine Transfor.	Using Kd-tree to build graphs and share learnable parameters
	O-CNN [177]	P	Octree	3DConv	Making 3D-CNN feasible for high-resolu. voxels
	PointCapsNet [233]	P	Enco.-deco.	PN	Semi-supervision learning
	SO-Net [97]	P	Enco.-deco.	FC layers	SOM for modeling spatial distribution + un-supervision learning

curves in point clouds to enhance point feature learning. PointMLP [118] introduces a lightweight geometric affine module to capture diverse geometric structures across different local regions. In the transformer domain, SPoTr [131] combines local self-attention and self-positioning global cross-attention to learn local and global features. Although Point Transformer has strong context-learning capabilities, its large number of parameters makes it challenging to achieve good performance on limited datasets.

Graph convolution is the most commonly used pipeline. SyncSpecCNN [218] introduces a synchronized spectral CNN to process irregular data in the spectral graph domain. In particular, multichannel and parametrized dilated convolution kernels are proposed to solve multi-scale analysis and information sharing across shapes, respectively. In the spatial graph domain, in analogy to a convolution kernel for images, KCNet [150] presents a point-set kernel and nearest-neighbor-graph to improve PointNet with an efficient local feature exploitation structure. Similarly, Wang et al. [175] design shape fully convolutional networks (SFCN) based on graph convolution and pooling operations, similar to FCN on images. SpiderCNN [209] applies a particular family of convolutional filters that combine simple step functions with Taylor polynomials, making the filters capture intricate local geometric variations effectively. Furthermore, FeaStNet [169] uses a dynamic graph convolution operator to build relationships between filter weights and graph neighborhoods instead of relying on the static graph of the above network.

A special kind of graph, the trees (e.g., Kd-tree and Octree), works on 3D shapes with different representations and can support various CNN architectures. Kd-Net [80]

uses a kd-tree data structure to represent point cloud connectivity. However, the networks have high computational costs. O-CNN [177] designs an Octree data structure from 3D shapes. However, the computational cost of the O-CNN grows quadratically as the depth of the tree increases.

SO-Net [97] sets up a self-organization map (SOM) from point clouds and hierarchically learns node-wise features on this map using the PointNet architecture. However, it fails to exploit local features fully. PartNet [221] decomposes 3D shapes top-down and proposes a Recursive Neural Network (RvNN) for learning the hierarchy of fine-grained parts. Zhao et al. [233] introduce an encoder-decoder network, 3D-PointCapsNet, to tackle several common point cloud-related tasks. The dynamic routing scheme and the peculiar 2D latent space deployed by capsule networks in their model bring improved performance. The 3D part segmentation methods are summarized in Table 6.

6. Applications

Deep learning based 3D segmentation technology holds significant value in cultural heritage preservation and semantic map construction.

6.1. Cultural Heritage Preservation

Cultural heritage preservation demands precise documentation of artifacts' shapes and textures for digital archiving, damage assessment, and research. Traditional methods of manual measurement and recording are often time-consuming and prone to errors. In contrast, deep learning based 3D segmentation provides an efficient and accurate

solution for capturing and analyzing detailed artifact information. Deep learning based 3D segmentation in cultural heritage preservation can generally be divided into the surface/object-level, and scene-level segmentation.

Surface/object-level segmentation: targets the segmentation of different surface types or textures, like walls, floors, or detailed carvings, to provide a detailed representation of structural features. Ganapathi et al. [38] develop a direct 3D mesh-based texture segmentation approach that identifies and classifies surface regions into texture and non-texture areas using a hybrid method combining classical features and a deep transformer. Furthermore, this team [37] introduces a binary classification framework that classifies texture and non-texture regions on 3D surfaces at the facet level using a deep vision transformer, with input generated from local geometric properties, demonstrating effectiveness on diverse texture pattern datasets. Ji et al. [72] develop a semantic segmentation and visualization framework that enhances the extraction of soft edges in cultural heritage reliefs using a deep learning based network, demonstrated on the Borobudur Temple bas-reliefs. They employ a novel opacity-based edge highlighting technique to extract soft edges, which are characteristic of reliefs, and incorporate them as guide information in a multichannel image input (including RGB, depth maps, and soft-edge images) to a custom network. Fu et al. [36] develop a Swin Transformer- and YOLOv5-based model for the automated classification, segmentation, and detection of surface defects in heritage buildings.

Scene-level segmentation: involves segmenting entire scenes or environments to understand the spatial context and layout of cultural heritage sites, capturing relationships between objects and features. Matrone et al. [120] make a comparative analysis of machine learning and deep learning methods for semantic segmentation of large 3D cultural heritage point clouds, and propose a hybrid architecture named DGCNN-Mod+3Dfeat, to enhance complex scene recognition. Pierdicca et al. [135] develop an enhanced deep learning framework for 3D point cloud segmentation in the Digital Cultural Heritage domain, utilizing an improved DGCNN that incorporates additional features like normal and color. Haznedar et al. [50] evaluate PointNet-based segmentation for heritage buildings, revealing its limitations with deformed and deteriorated structures, and propose a novel workflow that enhances segmentation accuracy by training PointNet with restitution-based synthetic data. Artopoulos et al. [3] integrate deep neural networks (DNNs) and support vector machines (SVMs) for identifying architectural stylistic influences in Cypriot historical architecture. Zhao et al. [230] propose a DSC-Net that leverages Enhanced Dual Attention Pooling and Global Context Feature Aggregation for precise 3D point cloud segmentation. Yang et al. [213] propose a novel network GSS-Net for point cloud semantic segmentation tailored for grotto scenes. This model incorporates knowledge guidance such as point cloud density, visual color, local geometric features, and global spatial distribution, to enhance segmentation accuracy.

6.2. 3D Semantic Map Construction

Unmanned systems do not just need to avoid obstacles but also need to establish a deeper understanding of the scene such as object parsing, self localization etc. To facilitate such tasks, unmanned systems build a 3D semantic map of the scene which includes two key problems: geometric reconstruction and semantic segmentation. 3D scene reconstruction has conventionally relied on simultaneous localization and mapping system (SLAM) to obtain a 3D map without semantic information. This is followed by semantic segmentation. 3D semantic map construction can be appropriate to categorize into non-real-time approaches and real-time approaches.

Non-real-time approaches: may be more suited for post-processing or tasks requiring high precision analysis. To obtain more information, some works learn the connections between frames to enhance the segmentation accuracy. For example, Xiang et al. [201] propose a data associated recurrent neural networks (DA-RNN) and integrate the output of the DA-RNN, which provides a consistent semantic labeling of the 3D scene. Cheng et al. [15] use a CRF-RNN-based semantic segmentation to generate the corresponding labels. Similarly, Kochanov et al. [81] also use scene flow to propagate dynamic objects within the 3D semantic maps. Some works fuse the multi-modal data to improve the segmentation accuracy. For example, Berrio et al. [100] integrate LIDAR and camera data to build a 3D semantic voxelized map, incorporating uncertainties in sensor readings and enhancing semantic segmentation for autonomous vehicle navigation. Shi et al. [7] improve 3D semantic map generation from RGB-D scans by focusing on accurate 2D frame labeling and combining them in 3D space using a novel semantic fusion mechanism, enhanced by a two-stream network and discriminatory mask loss for robust semantic segmentation.

Real-time approaches: are typically used in tasks requiring immediate environmental awareness, such as autonomous driving and robotic navigation. Qin et al. [140] introduce a cost-effective localization framework for autonomous driving that utilizes low-cost cameras and compact visual semantic maps, incorporating semantic segmentation to accurately identify road elements for improved localization. Wilson et al. [189] develop a MotionSC algorithm to leverage 3D deep learning to enhance SSC with temporal information, improving real-time dense local semantic mapping in dynamic environments. Wang et al. [173] introduce a real-time semantic mapping methodology that combines 2D and 3D networks within a SLAM system, enhancing image segmentation and 3D map processing, achieving state-of-the-art semantic mapping quality and superior cross-sensor generalization in real-time applications. Yamazaki et al. [210] develop a real-time open-vocabulary 3D mapping approach that uses a vision-language foundation model and TSDF for swift 3D scene reconstruction, achieving annotation-free 3D segmentation and superior performance in open-world semantics without additional 3D training.

Table 7

Evaluation performance regarding for RGB-D semantic segmentation methods on the SUN-RGB-D and NYUDv2. Note that the '%' after the value is omitted and the symbol '-' means the results are unavailable.

Methods	NYUDv2		SUN-RGB-D	
	mAcc	mIoU	mAcc	mIoU
Guo et al. [43]	46.3	34.8	45.7	33.7
Wang et al. [176]	–	44.2	–	–
Mousavian et al. [126]	52.3	39.2	–	–
Liu et al. [112]	50.8	39.8	50.0	39.4
Gupta et al. [45]	35.1	28.6	–	–
Liu et al. [111]	51.7	41.2	–	–
hazirbas et al. [49]	–	–	48.3	37.3
Lin et al. [107]	–	47.7	–	48.1
Jiang et al. [74]	–	–	50.6	39.3
Wang et al. [179]	47.3	–	–	–
Cheng et al. [16]	60.7	45.9	58.0	–
Fan et al. [32]	50.2	–	–	–
Li et al. [103]	49.4	–	48.1	–
Qi et al. [138]	55.7	43.1	57.0	45.9
Wang et al. [174]	60.6	38.3	50.1	33.5

7. Experimental Results

Below, we summarize the quantitative results of the segmentation methods discussed earlier on some typical public datasets and analyze these results qualitatively.

7.1. Results for 3D Semantic Segmentation

We report the results of RGB-D-based semantic segmentation methods on SUN-RGB-D [158] and NYUDv2 [156] datasets using mean accuracy (mA), overall accuracy (OA), and mean intersection over union (mIoU) as the evaluation metrics. These results of various methods are taken from the original articles and shown in Table 7.

We report the results of projected images, voxel, point clouds, and other representation semantic segmentation methods on S3DIS [2] (both Area 5 and 6-fold cross-validation), ScanNet [21] (test sets), Semantic3D [46] (reduced-8 subsets), and SemanticKITTI [5] (only xyz without RGB). We use mA, OA, and mIoU as the evaluation metrics. These results of various methods are taken from the original papers. Tables 8 reports the results.

Point cloud semantic segmentation architectures typically focus on five main components: basic framework, neighborhood search, features abstraction, coarsening, and pre-processing. Below, we provide a more detailed discussion of each component.

Basic framework: is one of the main driving forces behind the development of 3D segmentation. Generally, two main basic frameworks exist, including PointNet and PointNet++. The PointNet framework utilizes shared MLPs to capture point-wise features and employs max-pooling to aggregate these features into a global representation. However, it cannot learn local features due to the absence of a defined local neighborhood. Additionally, the fixed resolution of the feature map makes it challenging to adapt to deep architectures.

In contrast, the PointNet++ framework introduces a novel hierarchical learning architecture. It hierarchically defines local regions and progressively extracts features from these regions. This approach enables the network to capture local and global information, improving performance. As a result, many current networks adopt the PointNet++ framework or similar variations (such as 3D U-Net). This framework significantly reduces computational and memory complexities, particularly in high-level tasks like semantic segmentation, instance segmentation, and detection.

Neighborhood search: To exploit the local features of point clouds, neighborhood point search is introduced into networks, including the KNN [229], [142], [139], ball search [56], [166], [94], grid-based search [63], [195] and tree-based search [92]. KNN search retrieves the K closest neighbors to a query point based on a distance metric and hence lacks robustness to point clouds with varying densities. Some works integrate the dilated mechanism with the neighbor search to expand the receptive field [83], [101], [96]. Ball search involves finding all points within a specified radius (ball) around a query point. Similarly, grid-based search divides the point cloud space into a regular grid structure. Ball and grid-based algorithms are helpful for effectively capturing local structures and neighborhoods of varying densities.

Features abstraction: In feature abstraction, commonly used methods include MLP-based, convolution-based, and transformer-based approaches. MLP often extracts features from individual points in point cloud data. MLP learns nonlinear point-level feature representations by bypassing each point's feature vectors through multiple fully connected layers. MLP offers flexibility and scalability in point cloud processing. Convolution operations on point clouds typically involve aggregating (low-level) information from local points to capture local structures and contextual information. In contrast, transformer-based methods establish correlations between high-level point information through the attention mechanism, which is more helpful for high-level tasks such as point cloud segmentation. The essence of MLP-based, convolution-based, and transformer-based methods is to learn the relationships between points and obtain robust weights. In the context of a similar baseline architecture, the more comprehensive the learned point cloud relationship in the feature abstraction process, the stronger the robustness of the model becomes. Recently, MLP-based methods, such as Resurf [142] and PointNeXt [139], exhibit better accuracy and efficiency, encouraging researchers to re-examine and further explore the potential of MLP-based approaches.

Coarsening, also known as downsampling or subsampling, involves reducing the number of points in the point cloud while preserving the essential structures and features. Coarsening techniques include *random sampling* [60], *farthest point sampling* [136, 137], *tree-based* methods [92] and mesh-based decimation [95]. This step helps to reduce computational complexity and improve efficiency in subsequent stages of the segmentation process. Random sampling is

Table 8

Evaluation performance regarding for projected images, voxel, point clouds and other representation semantic segmentation methods on the S3DIS, ScanNet, Semantic3D and SemanticKITTI. Note: the ‘%’ after the value is omitted, the symbol ‘–’ means the results are unavailable, the dotted line means the subdivision of methods according to the type of architecture.

Method	Type	S3DIS			ScanNet		Semantic3D		SemanticKITTI	
		Area5	mIoU	6-fold	test set		reduced-8		only xyz	
		mAcc	mIoU	mIoU	oAcc	mIoU	oAcc	mIoU	mAcc	mIoU
Lawin et al. [90]	projection	–	–	–	–	–	88.9	58.5	–	–
Boulch et al. [9]		–	–	–	–	–	91.0	67.4	–	–
Wu et al. [190]		–	–	–	–	–	–	–	–	37.2
Wang et al. [183]		–	–	–	–	–	–	–	–	39.8
Wu et al. [191]		–	–	–	–	–	–	–	–	44.9
Milioto et al. [124]		–	–	–	–	–	–	–	–	52.2
Xu et al. [206]		–	–	–	–	–	–	–	–	55.9
RangViT [1]		–	–	–	–	–	–	–	–	55.9
RangFormer [84]		–	–	–	–	–	–	–	–	64.0
Tchapmi et al. [165]	voxel	57.35	48.92	48.92	–	–	88.1	61.30	–	–
Meng et al. [122]		–	78.22	–	–	–	–	–	–	–
Liu et al. [109]		–	70.76	–	–	–	–	–	–	–
PointNet [136]	point	48.98	41.09	47.71	–	14.69	–	–	29.9	17.9
G+RCU [31]		59.10	52.17	58.27	75.53	–	–	–	57.59	29.9
ESC [29]		54.06	45.14	49.7	63.4	–	–	–	40.9	26.4
HRNN [215]		71.3	53.4	–	76.5	–	–	–	49.2	34.5
PointNet++ [137]		–	50.04	54.4	71.40	34.26	–	–	–	–
PointWeb [228]		66.64	60.28	66.7	85.9	–	–	–	–	–
PointSIFT [76]		–	70.23	70.2	–	41.5	–	–	–	–
Resurf [142]		76.0	68.9	74.3	–	70.0	–	–	–	–
PointNeXt [139]		–	70.5	74.9	–	71.2	–	–	–	–
PointVector [24]		78.1	72.3	78.4	–	–	–	–	–	–
RSNet [65]		59.42	56.5	56.47	–	39.35	–	–	–	–
DPC [30]		68.38	61.28	–	–	59.2	–	–	–	–
PointwiseCNN [63]		56.5	–	–	–	–	–	–	–	–
PCCN [178]		67.01	58.27	–	–	49.8	–	–	–	–
PointCNN [101]		63.86	57.26	65.3	85.1	45.8	–	–	–	–
KPConv [167]		–	67.1	70.6	–	66.6	92.9	74.6	–	–
KPConvX [166]		78.7	73.5	–	–	76.3	–	–	–	–
PointConv [193]		–	50.34	–	–	55.6	–	–	–	–
A-CNN [83]		–	–	–	85.4	–	–	–	–	–
RandLA-Net [60]		–	–	70.0	–	–	94.8	77.4	–	53.9
PolarNet [226]		–	–	–	–	–	–	–	–	54.3
DGCNN [184]		–	56.1	56.1	–	–	–	–	–	–
SPG [89]		66.50	58.04	62.1	–	–	94.0	73.2	–	–
SPH3D-GCN [94]		65.9	59.5	68.9	–	61.0	–	–	–	–
DeepGCNs [96]		–	60.0	–	–	–	–	–	–	–
PointGCRNet [119]		–	52.43	–	–	60.8	–	–	–	–
AGCN [205]		–	–	56.63	–	–	–	–	–	–
PAN [34]		–	66.3	–	86.7	42.1	–	–	–	–
TGNet [102]		–	58.7	–	66.2	–	–	–	–	–
HDGCN [105]		65.81	59.33	66.85	–	–	–	–	–	–
3DContextNet [224]		74.5	55.6	55.6	–	–	–	–	–	–
PGCRNet [119]		–	54.4	–	–	–	–	69.5	–	–
AGCN [205]		74.5	55.6	55.6	–	–	–	–	–	–
PointANSL [211]		–	62.6	68.7	–	–	66.6	–	–	–
Point Transformer [229]		76.5	70.4	73.5	–	–	–	–	–	–
Point Transformer v2 [195]		77.9	71.6	–	–	75.2	–	–	–	–
FPTTransformer [55]		78.8	73.1	76.8	–	75.5	–	–	–	–
PatchFormer [225]		–	68.1	–	–	–	–	–	–	–
Fast Point Transformer [130]		77.3	70.1	–	–	–	–	–	–	–
Stratify Transformer [88]		78.1	72.0	–	–	73.7	–	–	–	–
SphereFormer [87]		–	–	–	–	–	–	–	–	78.4
ConDaFormer [25]		78.9	73.5	–	–	75.5	–	–	–	–
Point Transformer v3 [194]		80.1	74.3	80.8	78.6	79.4	–	–	–	75.5
TangentConv [164]	others	62.2	52.8	–	80.1	40.9	89.3	66.4	–	–
SPLATNet [160]		–	–	–	–	39.3	–	–	–	–
LatticeNet [147]		–	–	–	–	64.0	–	–	–	52.9
Hung et al. [17]		–	–	–	–	63.4	–	–	–	–
PVCNN [115]		87.12	58.98	–	–	–	–	–	–	–
MVPNet [70]		–	–	–	–	66.4	–	–	–	–
BPNNet [61]		–	–	–	–	74.9	–	–	–	–

simple and computationally efficient but may not select optimal points for maintaining local and global structures. This can potentially lead to information loss in feature-rich regions. FPS is widely used in networks to ensure a more even spatial distribution of the selected points and help

preserve global structures. However, local structures can still be destroyed with the farthest point sampling. Tree-based methods leverage hierarchical tree structures, such as an octree, to partition the point cloud and perform coarsening. Mesh-based methods must first convert the point cloud to a

Table 9

Evaluation performance regarding for 3D instance segmentation methods on the ScanNet. Note: the '%' after the value is omitted.

Methods	mAP	bath.	bed	book.	cabi.	chair	count.	curt.	desk	door	other	pict.	refr.	shower.	sink	sofa	table	toilet	wind.
GSPN [219]	30.6	50.0	40.5	31.1	34.8	58.9	5.4	6.8	12.6	28.3	29.0	2.8	21.9	21.4	33.1	39.6	27.5	82.1	24.5
3D-SIS [58]	38.2	100	43.2	24.5	19.0	57.7	1.3	26.3	3.3	32.0	24.0	7.5	42.2	85.7	11.7	69.9	27.1	88.3	23.5
3D-BoNet [212]	48.8	100	67.2	59.0	30.1	48.4	9.8	62.0	30.6	34.1	25.9	12.5	43.4	79.6	40.2	49.9	51.3	90.9	43.9
SGPN [180]	14.3	20.8	39.0	16.9	6.5	27.5	2.9	6.9	0	8.7	4.3	1.4	2.7	0	11.2	35.1	16.8	43.8	13.8
3D-MPA [28]	61.1	100	83.3	76.5	52.6	75.6	13.6	58.8	47.0	43.8	43.2	35.8	65.0	85.7	42.9	76.5	55.7	100	43.0
SoftGroup [170]	76.1	100	80.8	84.5	71.6	86.2	24.3	82.4	65.5	62.0	73.4	69.9	79.1	98.1	71.6	84.4	76.9	100	59.4
SSTNet [104]	69.8	100	69.7	88.8	55.6	80.3	38.7	62.6	41.7	55.6	58.5	70.2	60.0	100	82.4	72.0	69.2	100	50.9
3D-BEVIS [26]	24.8	66.7	56.6	7.6	3.5	39.4	2.7	3.5	9.8	9.8	3.0	2.5	9.8	37.5	12.6	60.4	18.1	85.4	17.1
PanopticFus. [127]	47.8	66.7	71.2	59.5	25.9	55.0	0	61.3	17.5	25.0	43.4	43.7	41.1	85.7	48.5	59.1	26.7	94.4	35.9
OccuSeg [47]	67.2	100	75.8	68.2	57.6	84.2	47.7	50.4	52.4	56.7	58.5	45.1	55.7	100	75.1	79.7	56.3	100	46.7
MTML [86]	54.9	100	80.7	58.8	32.7	64.7	0.4	81.5	18.0	41.8	36.4	18.2	44.5	100	44.2	68.8	57.1	100	39.6
PointGroup [75]	63.6	100	76.5	62.4	50.5	79.7	11.6	69.6	38.4	44.1	55.9	47.6	59.6	100	66.6	75.6	55.6	99.7	51.3
HAIS [13]	69.9	100	84.9	82.0	67.5	80.8	27.9	75.7	46.5	51.7	59.6	55.9	60.0	100	65.4	76.7	67.6	99.4	56.0
Dyco3D [52]	64.1	100	84.1	89.3	53.1	80.2	11.5	58.8	44.8	43.8	53.7	43.0	55.0	85.7	53.4	76.4	65.7	98.7	56.8
DKNet [196]	71.8	100	81.4	78.2	61.9	87.2	22.4	75.1	56.9	67.7	58.5	72.4	63.3	98.1	51.5	81.9	73.6	100	61.7
ISBNet [129]	76.3	100	87.3	71.7	66.6	85.8	50.8	66.7	76.4	64.3	67.6	68.8	82.5	100	77.3	74.1	77.7	100	55.6
Spherical Mask [154]	81.2	100	97.3	85.2	71.8	91.7	57.4	67.7	74.8	72.9	71.5	79.5	80.9	100	83.1	85.4	78.7	100	63.8
SPFormer [163]	77.0	90.3	90.3	80.6	60.9	88.6	56.8	81.5	70.5	71.1	65.5	65.2	68.5	100	78.9	80.9	77.6	100	58.3
Mask3D [149]	78.0	100	78.6	71.6	69.6	88.5	50.0	71.4	81.0	67.2	71.5	67.9	80.9	100	83.1	83.3	78.7	100	60.2
QueryFormer [117]	78.7	100	93.3	60.1	75.4	88.6	55.8	66.1	76.7	66.5	71.6	63.9	80.8	100	84.4	89.7	80.4	100	62.4
OneFormer [82]	80.1	100	97.3	90.9	69.8	92.8	58.2	66.8	68.5	78.0	68.7	69.8	70.2	100	79.4	90.0	78.4	98.6	63.5

mesh before it can be decimated. This adds computational overhead to the already expensive mesh decimation process. Moreover, creating a mesh from complex and sparse point clouds obtained from LiDAR sensors is not always possible [95].

The above methods are hand-crafted or engineered techniques that do not directly involve learning parameters from the data, which determines the sub-sampling pattern based on predefined rules or heuristics without explicitly optimizing for the task. Therefore, some works propose learnable coarsening methods that integrate a learnable layer into the coarsening module, such as pooling [41], [87], [195], [229], and attention mechanism [211].

Pre-processing: is an essential step in point cloud semantic segmentation that involves preparing and transforming the raw point cloud data before feeding it into the segmentation network. Pre-processing aims to enhance the data's quality, consistency, and suitability for the segmentation task. Some common pre-processing aspects of point cloud segmentation include data normalization, outlier removal, data augmentation, and point registration.

Point clouds often have varying scales, which can negatively affect the performance of segmentation networks. Data normalization involves scaling the point cloud data to a standard range or unit sphere to ensure consistent scales across different points. For example, the number of ShapNet object points is generally fixed at 4096. For the complexity scene, early works [208], [136] divided raw point clouds into smaller ones (e.g., 4096 points, 1m³ blocks) so that the processing does not require large memory. However, this strategy might break down the semantic continuity of the scene. Recent works [139], [87], [195], [229], [95] input the complete scene into the network, but that requires

more computational sources. Moreover, these works tend to downsample the point cloud in the pre-processing stage.

7.2. Results for 3D Instance Segmentation

We report the results of 3D instance segmentation methods on ScanNet [21] datasets and choose mAP as the evaluation metrics. The results of these methods are taken from the ScanNet Benchmark Challenge website, shown in Table 9 and summarized in Figure 9. The Spherical Mask [154] has state-of-the-art performance, with 81.2% average precision on the ScanNet dataset at this view. It also achieves the best instance segmentation performance in most classes, including 'bathtub,' 'shower curtain,' 'toilet,' and so on.

Most methods have better segmentation performance on large-scale classes such as 'bathtub' and 'toilet' and have poor segmentation performance on small-scale classes such as 'counter,' 'desk,' and 'picture.' Therefore, the instance segmentation of small objects is a prominent challenge.

In proposal-based methods, specifically the 2D embedding propagating-based methods such as 3D-BEVIS [26] and PanopticFusion [127], they tend to exhibit poorer performance compared to other proposal-free methods. This is primarily because simple embedding propagation techniques are more susceptible to error labels, leading to inaccuracies in the instance segmentation results.

Proposal-free methods demonstrate superior performance than proposal-based methods in instance segmentation across all classes, particularly for small objects like 'curtains,' 'pictures,' 'shower curtains,' and 'sinks.' Unlike proposal-based methods that rely on the accuracy of proposal generation, proposal-free methods circumvent this issue entirely. They directly consider the entire point cloud and its global features, enabling more precise and comprehensive instance segmentation. By avoiding the need for proposal generation,

Table 10

Evaluation performance regarding for 3D part segmentation on the ShapeNet. Note: the '%' after the value is omitted, the symbol '-' means the results are unavailable.

Methods	Ins. mIoU	Methods	Ins. mIoU
VV-Net [122]	87.4	LatticeNet [160]	83.9
SSCNet [40]	86.0	SGPN [180]	85.8
PointNet [136]	83.7	ShapePFCN [78]	88.4
PointNet++ [137]	85.1	VoxSegNet [185]	87.5
3DContextNet [224]	84.3	Pointgrid[91]	86.4
RSNet [65]	84.9	KPConv [166]	86.4
MCC [56]	85.9	SO-Net [97]	84.9
PointConv [193]	85.7	PartNet [221]	87.4
DGCNN [184]	85.1	SyncSpecCNN [218]	84.7
SPH3D-GCN [94]	86.8	KCNet [218]	84.7
AGCN [205]	85.4	PointCNN [101]	86.1
PCCN [178]	85.9	SpiderCNN [209]	85.3
Flex-Conv [41]	85.0	FeaStNet [169]	81.5
ψ -CNN [92]	86.8	Kd-Net [80]	82.3
SPLATNet [160]	84.6	O-CNN [177]	85.9
DRGCNN [223]	86.2	PointVector [24]	86.9
SPoTr [131]	87.2	PointNext [139]	87.1
CurveNet [200]	86.8	PointMLP [118]	86.1
Point Transformer [229]	86.6		

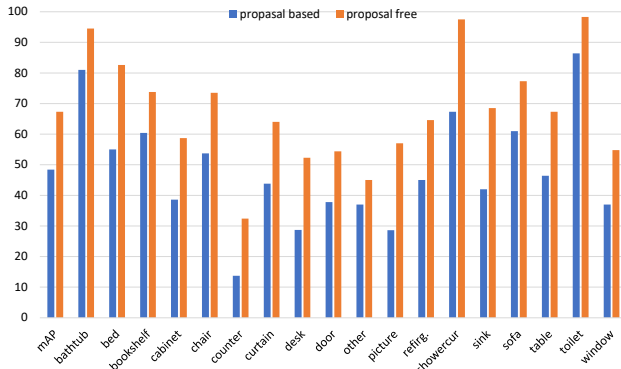


Fig. 9: Evaluation performance regarding for 3D instance segmentation architecture, including proposal based and proposal free, on the different class of ScanNet. For simplicity, we omit the '%' after the value.

proposal-free methods can achieve better results by considering the overall context and characteristics of the point cloud.

7.3. Results for 3D Part Segmentation

We report the results of 3D part segmentation methods on ShapeNet [217] datasets and use Ins. mIoU as the evaluation metric. These results of various techniques are taken from the original papers and shown in Table 10. We can find that the part segmentation performance of all methods is quite similar. One underlying assumption is that objects in ShapeNet datasets are synthetic, normalized in scale, aligned in pose, and lack scene context. This makes it difficult for part segmentation networks to extract rich context features. Another underlying assumption is that the point clouds in the

synthetic scenes without background noise are simpler and cleaner than the ones in the real scenes, so the geometric features of point clouds are easy to exploit. The accuracy performance of various part segmentation networks is challenging to distinguish effectively.

8. Challenges and Discussions

3D segmentation using deep learning techniques has made significant progress in recent years. However, this is just the beginning, and considerable challenges lie ahead. Below, we present some challenges and identify potential research directions.

Data Scarcity and Quality: Annotated 3D datasets are less abundant than 2D image datasets, This is because creating high-quality 3D annotations requires significant time and expertise, limiting the availability of large-scale datasets for training deep learning models. 3D data from various sensors often contain noise, missing regions, and inconsistencies. These issues pose significant challenges for accurate segmentation. Below, we list some promising research directions aimed at addressing this challenge.

- *Synthetic data generation* gradually plays an important role in 3D segmentation due to the low cost and diverse scenes that can be generated [10], [197] compared to real dataset. Besides, Synthetic data can include detailed important semantic information, such as material and texture information, which is essential for segmentation with similar color or geometric information.
- *Transfer Learning* involves leveraging pre-trained models to improve performance on specific tasks, where the models are generally trained on large, often unrelated datasets [192], [234]. In the context of 3D segmentation, transfer learning can significantly enhance accuracy performance and address challenges related to data scarcity and quality.
- *Weakly-Supervised Learning* minimizes the need for extensive and precise annotations by using less detailed supervision. This approach effectively reduces annotation effort while still improving model training. It addresses data scarcity by making use of weaker or less accurate labels [162], [152], [85], and it helps manage data quality by being resilient to imperfections in the provided labels.
- *Semi-Supervised Learning* combines labeled and unlabeled data to enhance model performance and lower annotation costs [99]. By leveraging a small amount of labeled data along with a larger pool of unlabeled data, this method improves generalization and robustness. It is particularly effective in situations where labeled data is limited but a larger volume of unlabeled data is available.

- *Unsupervised Learning* operates without labeled data, focusing on discovering hidden structures and patterns within the data [227], [203]. This approach is highly adaptable and resilient to data quality issues, making it ideal for scenarios with limited or noisy data [202]. It learns valuable representations and insights from the data itself, without relying on annotated labels.

Generalization and Robustness: Models trained on specific datasets may not generalize well to different types of 3D data, such as those acquired from different sensors or environments. Developing robust models that perform well across various domains remains a challenge. Besides, Variations in object shapes, sizes, and orientations in real-world can affect model performance. Ensuring robustness to such variations is critical for reliable 3D segmentation. Below we list promising research directions for improving the generalization and robustness of point cloud processing.

- *Domain Adaptation* is a technique used to adapt models so they can perform effectively across different domains or environments, especially when there is a shift or discrepancy between the source domain and the target domain [232], [216]. Domain adaptation technique, including aligning features, reweighing instances, fine-tuning and self-training, is especially important in scenarios where labeled data in the target domain is limited or unavailable.
- *Multi-Modal Approaches* use data from multiple sensor modalities (e.g., LiDAR, image, voice, language) to enhance robustness and generalization. By integrating diverse sources of information, these approaches provide a more comprehensive understanding of the environment [61], [98]. This integration helps mitigate the limitations of individual modalities, offering richer feature representations and better handling of variability and uncertainty.
- *Large Model Approaches* often have deeper architectures and more parameters, allowing them to capture complex features and patterns. Popular approaches can include segmenting point clouds with large image models (such as SAM [79], [188]) and natural language models like ChatGPT. The advanced capabilities of large models enable them to capture intricate patterns and semantic relationships, leading to improved performance and accuracy in segmentation tasks.
- *Meta-Learning* trains models to adapt rapidly to new, unseen data with minimal additional training [231]. By optimizing the learning process and leveraging prior knowledge from various tasks, meta-learning enhances a model's ability to generalize, perform well with few examples, and transfer knowledge across different tasks.

Computational Complexity: Processing 3D data is computationally intensive due to its high dimensionality and volume. Training deep learning models on 3D datasets requires substantial computational resources, including powerful GPUs and extensive memory. As the size and resolution of 3D data increase, scalability becomes a concern. Efficiently managing memory and computational resources is essential for handling large-scale 3D datasets. Below, we list promising research directions for improving the computational efficiency of models.

- *Efficient Architectures* aim to balance computational efficiency with high performance. Techniques such as sparse representations learning [143], and neural architecture search [60] help achieve this balance by reducing resource requirements while maintaining effective segmentation capabilities. These optimizations are crucial for deploying 3D segmentation models in scenarios.
- *Parallel Computing* leverages multiple processing units to handle the large-scale computations required for segmenting 3D data efficiently. Techniques such as multi-core CPUs, GPUs, distributed computing, and parallel algorithms help improve processing speed, scalability, and efficiency. This approach is crucial for applications that require real-time processing and accurate segmentation of complex 3D datasets.
- *Model Compression* involves techniques such as pruning, quantization, knowledge distillation [59], [71], low-rank factorization, efficient network design, and model sharing to reduce model size and computational requirements while preserving performance. These methods help make 3D segmentation models more practical and efficient for deployment in resource-constrained environments and applications that require real-time processing.

Interpretability and Explainability: Deep learning models for 3D segmentation, particularly those with complex architectures, often lack interpretability [4]. Understanding the decision-making process of these models is crucial for gaining trust and ensuring reliable deployment in critical applications. Providing clear and understandable explanations for segmentation results is important, especially in fields such as medical imaging and cultural heritage preservation, where decisions must be transparent and justifiable. Some promising research directions for improving interpretability and explainability of deep learning models are listed below.

- *Explainable AI (XAI) Methods* include visualization techniques (saliency and activation maps), attention mechanisms, feature visualization, surrogate models, rule-based explanations, counterfactual explanations, and layer-wise relevance propagation. These methods enhance the interpretability and transparency of 3D segmentation models by providing insights into how

decisions are made and which features are most influential. This facilitates better understanding, trust, and usability of AI systems across various applications.

- *Visualization and Post-Hoc Analysis* involve techniques such as saliency maps, activation maps, attention maps, feature visualization, surrogate models, rule-based explanations, counterfactual explanations. These methods help analyze and visualize model predictions and decision processes, offering insights into how 3D segmentation models work and enabling better understanding, debugging, and refinement of AI systems.
- *Interactive Tools* are specialized interfaces designed to help users visualize, explore, and understand the outputs of 3D segmentation models. Given the complexity of 3D data and the outputs of segmentation models, these tools are essential for gaining insights and making informed decisions about model performance and data interpretation.

9. Conclusion

In conclusion, we present a comprehensive survey of recent developments in 3D segmentation utilizing deep learning techniques. Through this survey, we devolved into 3D semantic segmentation, 3D instance segmentation, and 3D part segmentation; we have covered around 180 methodologies, each with its strengths and weaknesses. Our performance comparison highlights the current state-of-the-art approaches, offering valuable insights into their efficacy across different datasets and application scenarios. However, it's important to note that the field is dynamic, and new methods are continually emerging, promising even greater accuracy, efficiency, and versatility advancements. Moreover, we have identified several promising research directions for further investigation. These include the exploration of novel architectures tailored specifically for 3D segmentation tasks, integrating multi-modal data sources to enhance segmentation accuracy, and the development of techniques for handling large-scale and dynamic 3D environments. By pushing the boundaries of 3D segmentation research, we can unlock new possibilities across a wide range of domains, from medical imaging and robotics to autonomous driving and virtual reality. Utilizing recent advances in generative AI, we can tackle the complexities of 3D data and advance 3D segmentation.

References

- [1] Ando, A., Gidaris, S., Bursuc, A., Puy, G., Boulch, A., Marlet, R., 2023. Rangevit: Towards vision transformers for 3d semantic segmentation in autonomous driving, in: Proc. IEEE Conf. Comput. Vis. Pattern Recognit., pp. 5240–5250.
- [2] Armeni, I., Sener, O., Zamir, A., Jiang, H., Brilakis, I., Fischer, M., Savarese, S., 2016. 3d semantic parsing of large-scale indoor spaces, in: Proc. IEEE Conf. Comput. Vis. Pattern Recognit., pp. 1534–1543.
- [3] Artopoulos, G., Maslioukova, M.I., Zavou, C., Loizou, M., Deligiorgi, M., Averkiou, M., 2023. An artificial neural network framework for classifying the style of cypriot hybrid examples of built heritage in 3d. *Journal of Cultural Heritage* 63, 135–147.
- [4] Atik, M.E., Duran, Z., Seker, D.Z., 2024. Explainable artificial intelligence for machine learning-based photogrammetric point cloud classification. *IEEE Journal of Selected Topics in Applied Earth Observations and Remote Sensing*.
- [5] Behley, J., Garbade, M., Milioto, A., Quenzel, J., Behnke, S., Stachniss, C., Gall, J., 2019. Semantickitti: A dataset for semantic scene understanding of lidar sequences, in: Proc. IEEE Int. Conf. Computer Vis., IEEE. pp. 9297–9307.
- [6] Bello, S., Yu, S., Wang, C., Adam, J., Li, J., 2020. deep learning on 3d point clouds. *Remote Sens.* 12, 1729.
- [7] Berrio, J.S., Shan, M., Worrall, S., Nebot, E., 2021. Camera-lidar integration: Probabilistic sensor fusion for semantic mapping. *IEEE Transactions on Intelligent Transportation Systems* 23, 7637–7652.
- [8] Boulch, A., Guerry, J., Le Saux, B., Audebert, N., 2018. Snapnet: 3d point cloud semantic labeling with 2d deep segmentation networks. *Comput. Graph.* 71, 189–198.
- [9] Boulch, A., Le Saux, B., Audebert, N., 2017. Unstructured point cloud semantic labeling using deep segmentation networks. *3dor@eurographics* 2, 7.
- [10] Brodeur, S., Perez, E., Anand, A., Golemo, F., Celotti, L., Strub, F., Rouat, J., Larochelle, H., Courville, A., 2017. Home: A household multimodal environment. *arXiv preprint arXiv:1711.11017*.
- [11] Cao, Y., Shen, C., Shen, H., 2016. Exploiting depth from single monocular images for object detection and semantic segmentation. *IEEE Trans. Image Process.* 26, 836–846.
- [12] Chang, A., Dai, A., Funkhouser, T., Halber, M., Niebner, M., Savva, M., Song, S., Zeng, A., Zhang, Y., 2017. Matterport3d: Learning from rgb-d data in indoor environments, in: Proc. Int. Conf. 3D Vis., IEEE. pp. 667–676.
- [13] Chen, S., Fang, J., Zhang, Q., Liu, W., Wang, X., 2021. Hierarchical aggregation for 3d instance segmentation, in: Proc. IEEE Int. Conf. Comput. Vis., pp. 15467–15476.
- [14] Chen, X., Golovinskiy, A., Funkhouser, T., 2009. A benchmark for 3d mesh segmentation. *ACM Trans. Graph.* 28, 1–12.
- [15] Cheng, J., Sun, Y., Meng, M.Q.H., 2020. Robust semantic mapping in challenging environments. *Robotica* 38, 256–270.
- [16] Cheng, Y., Cai, R., Li, Z., Zhao, X., Huang, K., 2017. Locality-sensitive deconvolution networks with gated fusion for rgb-d indoor semantic segmentation, in: Proc. IEEE Conf. Comput. Vis. Pattern Recognit., pp. 3029–3037.
- [17] Chiang, H.Y., Lin, Y.L., Liu, Y.C., Hsu, W.H., 2019. A unified point-based framework for 3d segmentation, in: Proc. Int. Conf. 3D Vis., IEEE. pp. 155–163.
- [18] Chollet, F., 2017. Xception: Deep learning with depthwise separable convolutions, in: Proc. IEEE Conf. Comput. Vis. Pattern Recognit., pp. 1251–1258.
- [19] Choy, C., Gwak, J., Savarese, S., 2019. 4d spatio-temporal convnets: Minkowski convolutional neural networks, in: Proc. IEEE Conf. Comput. Vis. Pattern Recognit., pp. 3075–3084.
- [20] Couprie, C., Farabet, C., Najman, L., LeCun, Y., 2013. Indoor semantic segmentation using depth information. *arXiv preprint arXiv:1301.3572*.
- [21] Dai, A., Chang, A., Savva, M., Halber, M., Funkhouser, T., Nießner, M., 2017. Scannet: Richly-annotated 3d reconstructions of indoor scenes, in: Proc. IEEE Conf. Comput. Vis. Pattern Recognit., pp. 5828–5839.
- [22] Dai, A., Nießner, M., 2018. 3dmv: Joint 3d-multi-view prediction for 3d semantic scene segmentation, in: Proc. Eur. Conf. on Comput. Vis., Springer. pp. 452–468.
- [23] Dai, A., Ritchie, D., Bokeloh, M., Reed, S., Sturm, J., Nießner, M., 2018. Scancomplete: Large-scale scene completion and semantic segmentation for 3d scans, in: Proc. IEEE Conf. Comput. Vis. Pattern Recognit., pp. 4578–4587.

- [24] Deng, X., Zhang, W., Ding, Q., Zhang, X., 2023. Pointvector: a vector representation in point cloud analysis, in: Proceedings of the IEEE/CVF Conference on Computer Vision and Pattern Recognition, pp. 9455–9465.
- [25] Duan, L., Zhao, S., Xue, N., Gong, M., Xia, G.S., Tao, D., 2024. Condaformer: Disassembled transformer with local structure enhancement for 3d point cloud understanding. *Advances in Neural Information Processing Systems* 36.
- [26] Elich, C., Engelmann, F., Kontogianni, T., Leibe, B., 2019. 3d bird's-eye-view instance segmentation, in: German Conf. Pattern Recognit., Springer. pp. 48–61.
- [27] Emre Yurdakul, E., Yemez, Y., 2017. Semantic segmentation of rgb-d videos with recurrent fully convolutional neural networks, in: Proc. IEEE Int. Conf. Computer Vis. Worksh., pp. 367–374.
- [28] Engelmann, F., Bokeloh, M., Fathi, A., Leibe, B., Nießner, M., 2020a. 3d-mpa: Multi-proposal aggregation for 3d semantic instance segmentation, in: Proc. IEEE Conf. Comput. Vis. Pattern Recognit., pp. 9031–9040.
- [29] Engelmann, F., Kontogianni, T., Hermans, A., Leibe, B., 2017. Exploring spatial context for 3d semantic segmentation of point clouds, in: Proc. IEEE Int. Conf. Computer Vis. Worksh., pp. 716–724.
- [30] Engelmann, F., Kontogianni, T., Leibe, B., 2020b. Dilated point convolutions: On the receptive field size of point convolutions on 3d point clouds, in: Proc. IEEE Int. Conf. Robot. Autom., IEEE. pp. 9463–9469.
- [31] Engelmann, F., Kontogianni, T., Schult, J., Leibe, B., 2018. Know what your neighbors do: 3d semantic segmentation of point clouds, in: Proc. Eur. Conf. on Comput. Vis., Springer. pp. 0–0.
- [32] Fan, H., Mei, X., Prokhorov, D., Ling, H., 2017. Rgb-d scene labeling with multimodal recurrent neural networks, in: Proc. IEEE Conf. Comput. Vis. Pattern Recognit. Worksh., pp. 9–17.
- [33] Fan, H., Yang, Y., Kankanhalli, M., 2021. Point 4d transformer networks for spatio-temporal modeling in point cloud videos, in: Proc. IEEE Conf. Comput. Vis. Pattern Recognit., pp. 14204–14213.
- [34] Feng, M., Zhang, L., Lin, X., Gilani, S.Z., Mian, A., 2020. Point attention network for semantic segmentation of 3d point clouds. *Pattern Recognit.* , 107446.
- [35] Fooladgar, F., Kasaei, S., 2020. A survey on indoor rgb-d semantic segmentation: from hand-crafted features to deep convolutional neural networks. *Multimed. Tools. Appl.* 79, 4499–4524.
- [36] Fu, X., Angkawisittpan, N., 2024. Detecting surface defects of heritage buildings based on deep learning. *Journal of Intelligent Systems* 33, 20230048.
- [37] Ganapathi, I.I., Ali, S.S., Owais, M., Gour, N., Javed, S., Werghe, N., 2023. Facet-level segmentation of 3d textures on cultural heritage objects, in: 2023 IEEE International Conference on Image Processing (ICIP), IEEE. pp. 3035–3039.
- [38] Ganapathi, I.I., Javed, S., Hassan, T., Werghe, N., 2022. Detecting 3d texture on cultural heritage artifacts, in: International Conference on Pattern Recognition, Springer. pp. 3–14.
- [39] Geiger, A., Lenz, P., Urtasun, R., 2012. Are we ready for autonomous driving? the kitti vision benchmark suite, in: Proc. IEEE Conf. Comput. Vis. Pattern Recognit., IEEE. pp. 3354–3361.
- [40] Graham, B., Engelcke, M., Van Der Maaten, L., 2018. 3d semantic segmentation with submanifold sparse convolutional networks, in: Proc. IEEE Conf. Comput. Vis. Pattern Recognit., pp. 9224–9232.
- [41] Groh, F., Wieschollek, P., Lensch, H.P., 2018. Flex-convolution, in: Asian Conf. Comput. Vis., Springer. pp. 105–122.
- [42] Guerry, J., Boulch, A., Le Saux, B., Moras, J., Plyer, A., Filliat, D., 2017. Snapnet-r: Consistent 3d multi-view semantic labeling for robotics, in: Proc. IEEE Int. Conf. Computer Vis. Worksh., pp. 669–678.
- [43] Guo, Y., Chen, T., 2018. Semantic segmentation of rgb-d images based on deep depth regression. *Pattern Recognit. Lett.* 109, 55–64.
- [44] Guo, Y., Wang, H., Hu, Q., Liu, H., Liu, L., Bennamoun, M., 2020. Deep learning for 3d point clouds: A survey. *IEEE Trans. Pattern Anal. Mach. Intell.* 43, 4338–4364.
- [45] Gupta, S., Girshick, R., Arbeláez, P., Malik, J., 2014. Learning rich features from rgb-d images for object detection and segmentation, in: Proc. Eur. Conf. Comput. Vis., Springer. pp. 345–360.
- [46] Hackel, T., Savinov, N., Ladicky, L., Wegner, J., Schindler, K., Pollefeys, M., 2017. Semantic3d. net: A new large-scale point cloud classification benchmark. *arXiv preprint arXiv:1704.03847* .
- [47] Han, L., Zheng, T., Xu, L., Fang, L., 2020. Occseg: Occupancy-aware 3d instance segmentation, in: Proc. IEEE Conf. Comput. Vis. Pattern Recognit., pp. 2940–2949.
- [48] Hanocka, R., Hertz, A., Fish, N., Giryas, R., Fleishman, S., D., C.O., 2019. Meshcnn: a network with an edge. *ACM Trans. Graph.* 38, 1–12.
- [49] Hazirbas, C., Ma, L., Domokos, C., Cremers, D., 2016. Fusetnet: Incorporating depth into semantic segmentation via fusion-based cnn architecture, in: Proc. Asian Conf. Comput. Vis., Springer. pp. 213–228.
- [50] Haznedar, B., Bayraktar, R., Ozturk, A.E., Arayici, Y., 2023. Implementing pointnet for point cloud segmentation in the heritage context. *Heritage Science* 11, 2.
- [51] He, K., Gkioxari, G., Dollár, P., Girshick, R., 2017a. Mask r-cnn, in: Proc. IEEE Int. Conf. Computer Vis., pp. 2961–2969.
- [52] He, T., Shen, C., Van Den Hengel, A., 2021. Dyco3d: Robust instance segmentation of 3d point clouds through dynamic convolution, in: Proc. IEEE Conf. Comput. Vis. Pattern Recognit., pp. 354–363.
- [53] He, T., Yin, W., Shen, C., van den Hengel, A., 2022. Pointinst3d: Segmenting 3d instances by points, in: Proc. Eur. Conf. on Comput. Vis., Springer. pp. 286–302.
- [54] He, Y., Chiu, W.C., Keuper, M., Fritz, M., 2017b. Std2p: Rgb-d semantic segmentation using spatio-temporal data-driven pooling, in: Proc. IEEE Conf. Comput. Vis. Pattern Recognit., pp. 4837–4846.
- [55] He, Y., Yu, H., Yang, Z., Liu, X., Sun, W., Mian, A., 2024. Full point encoding for local feature aggregation in 3-d point clouds. *IEEE Transactions on Neural Networks and Learning Systems* .
- [56] Hermosilla, P., Ritschel, T., Vázquez, P.P., Vinacua, À., Ropinski, T., 2018. Monte carlo convolution for learning on non-uniformly sampled point clouds. *ACM Trans. Graph.* 37, 1–12.
- [57] Höft, N., Schulz, H., Behnke, S., 2014. Fast semantic segmentation of rgb-d scenes with gpu-accelerated deep neural networks, in: Joint German/Austrian Conf. on Artif. Intell., Springer. pp. 80–85.
- [58] Hou, J., Dai, A., Nießner, M., 2019. 3d-sis: 3d semantic instance segmentation of rgb-d scans, in: Proc. IEEE Conf. Comput. Vis. Pattern Recognit., pp. 4421–4430.
- [59] Hou, Y., Zhu, X., Ma, Y., Loy, C.C., Li, Y., 2022. Point-to-voxel knowledge distillation for lidar semantic segmentation, in: Proceedings of the IEEE/CVF conference on computer vision and pattern recognition, pp. 8479–8488.
- [60] Hu, Q., Yang, B., Xie, L., Rosa, S., Guo, Y., Wang, Z., Trigoni, N., Markham, A., 2020. Randa-net: Efficient semantic segmentation of large-scale point clouds, in: Proc. IEEE Conf. Comput. Vis. Pattern Recognit., pp. 11108–11117.
- [61] Hu, W., Zhao, H., Jiang, L., Jia, J., Wong, T.T., 2021. Bidirectional projection network for cross dimension scene understanding, in: Proc. IEEE Conf. Comput. Vis. Pattern Recognit., pp. 14373–14382.
- [62] Hua, B., Pham, Q., Nguyen, D., Tran, M., Yu, L., Yeung, S., 2016. Scenenn: A scene meshes dataset with annotations, in: Proc. Int. Conf. 3D Vis., IEEE. pp. 92–101.
- [63] Hua, B.S., Tran, M.K., Yeung, S.K., 2018. Pointwise convolutional neural networks, in: Proc. IEEE Conf. Comput. Vis. Pattern Recognit., pp. 984–993.
- [64] Huang, J., You, S., 2016. Point cloud labeling using 3d convolutional neural network, in: Proc. Int. Conf. Pattern Recognit., IEEE. pp. 2670–2675.
- [65] Huang, Q., Wang, W., Neumann, U., 2018. Recurrent slice networks for 3d segmentation of point clouds, in: Proc. IEEE Conf. Comput. Vis. Pattern Recognit., pp. 2626–2635.

- [66] Iandola, F., Han, S., Moskewicz, M., Ashraf, K., Dally, W., Keutzer, K., 2016. Squeezenet: Alexnet-level accuracy with 50x fewer parameters and < 0.5 mb model size. arXiv preprint arXiv:1602.07360.
- [67] Ioannidou, A., Chatzilari, E., Nikolopoulos, S., Kompatsiaris, I., 2017. Deep learning advances in computer vision with 3d data: A survey. *ACM Comput. Surv.* 50, 1–38.
- [68] Ivanek, B.J., 2016. Depth estimation by convolutional neural networks. Ph.D. thesis. Master thesis, Brno University of Technology.
- [69] Jampani, V., Kiefel, M., Gehler, P.V., 2016. Learning sparse high dimensional filters: Image filtering, dense crfs and bilateral neural networks, in: *Proc. IEEE Conf. Comput. Vis. Pattern Recognit.*, pp. 4452–4461.
- [70] Jaritz, M., Gu, J., Su, H., 2019. Multi-view pointnet for 3d scene understanding, in: *Proc. IEEE Int. Conf. Computer Vis. Works.*, pp. 0–0.
- [71] Ji, D., Wang, H., Tao, M., Huang, J., Hua, X.S., Lu, H., 2022. Structural and statistical texture knowledge distillation for semantic segmentation, in: *Proceedings of the IEEE/CVF Conference on Computer Vision and Pattern Recognition*, pp. 16876–16885.
- [72] Ji, S., Pan, J., Li, L., Hasegawa, K., Yamaguchi, H., Thufail, F.I., Brahmantara, Sarjiati, U., Tanaka, S., 2023. Semantic segmentation for digital archives of borobudur reliefs based on soft-edge enhanced deep learning. *Remote Sensing* 15, 956.
- [73] Jiang, H., Yan, F., Cai, J., Zheng, J., Xiao, J., 2020a. End-to-end 3d point cloud instance segmentation without detection, in: *Proc. IEEE Conf. Comput. Vis. Pattern Recognit.*, pp. 12796–12805.
- [74] Jiang, J., Zhang, Z., Huang, Y., Zheng, L., 2017. Incorporating depth into both cnn and crf for indoor semantic segmentation, in: *Proc. IEEE Int. Conf. Softw. Eng. Serv. Sci.*, IEEE. pp. 525–530.
- [75] Jiang, L., Zhao, H., Shi, S., Liu, S., Fu, C., Jia, J., 2020b. Pointgroup: Dual-set point grouping for 3d instance segmentation, in: *Proc. IEEE Conf. Comput. Vis. Pattern Recognit.*, pp. 4867–4876.
- [76] Jiang, M., Wu, Y., Zhao, T., Zhao, Z., Lu, C., 2018. Pointsift: A sift-like network module for 3d point cloud semantic segmentation. arXiv preprint arXiv:1807.00652.
- [77] Jing, L., Xue, Y., Yan, X., Zheng, C., Wang, D., Zhang, R., Wang, Z., Fang, H., Zhao, B., Li, Z., 2024. X4d-sceneformer: Enhanced scene understanding on 4d point cloud videos through cross-modal knowledge transfer, in: *Proceedings of the AAAI Conference on Artificial Intelligence*, pp. 2670–2678.
- [78] Kalogerakis, E., Averkiou, M., Maji, S., Chaudhuri, S., 2017. 3d shape segmentation with projective convolutional networks, in: *Proc. IEEE Conf. Comput. Vis. Pattern Recognit.*, pp. 3779–3788.
- [79] Kirillov, A., Mintun, E., Ravi, N., Mao, H., Rolland, C., Gustafson, L., Xiao, T., Whitehead, S., Berg, A.C., Lo, W.Y., et al., 2023. Segment anything. arXiv preprint arXiv:2304.02643.
- [80] Klovov, R., Lempitsky, V., 2017. Escape from cells: Deep kd-networks for the recognition of 3d point cloud models, in: *Proc. IEEE Int. Conf. Computer Vis.*, pp. 863–872.
- [81] Kochanov, D., Ošep, A., Stücker, J., Leibe, B., 2016. Scene flow propagation for semantic mapping and object discovery in dynamic street scenes, in: *Proc. IEEE Int. Conf. Intell. Rob. Syst.*, IEEE. pp. 1785–1792.
- [82] Kolodiazny, M., Vorontsova, A., Konushin, A., Rukhovich, D., 2024. Oneformer3d: One transformer for unified point cloud segmentation, in: *Proceedings of the IEEE/CVF Conference on Computer Vision and Pattern Recognition*, pp. 20943–20953.
- [83] Komarichev, A., Zhong, Z., Hua, J., 2019. A-cnn: Annularly convolutional neural networks on point clouds, in: *Proc. IEEE Conf. Comput. Vis. Pattern Recognit.*, pp. 7421–7430.
- [84] Kong, L., Liu, Y., Chen, R., Ma, Y., Zhu, X., Li, Y., Hou, Y., Qiao, Y., Liu, Z., 2023. Rethinking range view representation for lidar segmentation. arXiv preprint arXiv:2303.05367.
- [85] Kwon, H., Kim, J., Yoon, K.J., 2024. Weakly supervised point cloud semantic segmentation via artificial oracle, in: *Proceedings of the IEEE/CVF Conference on Computer Vision and Pattern Recognition*, pp. 3721–3731.
- [86] Lahoud, J., Ghanem, B., Pollefeys, M., Oswald, M., 2019. 3d instance segmentation via multi-task metric learning, in: *Proc. IEEE Int. Conf. Computer Vis.*, pp. 9256–9266.
- [87] Lai, X., Chen, Y., Lu, F., Liu, J., Jia, J., 2023. Spherical transformer for lidar-based 3d recognition, in: *Proc. IEEE Conf. Comput. Vis. Pattern Recognit.*, pp. 17545–17555.
- [88] Lai, X., Liu, J., Jiang, L., Wang, L., Zhao, H., Liu, S., Qi, X., Jia, J., 2022. Stratified transformer for 3d point cloud segmentation, in: *Proc. IEEE Conf. Comput. Vis. Pattern Recognit.*, pp. 8500–8509.
- [89] Landrieu, L., Simonovsky, M., 2018. Large-scale point cloud semantic segmentation with superpoint graphs, in: *Proc. IEEE Conf. Comput. Vis. Pattern Recognit.*, pp. 4558–4567.
- [90] Lawin, F., Danelljan, M., Tosteberg, P., Bhat, G., Khan, F., Felsberg, M., 2017. Deep projective 3d semantic segmentation, in: *Comput. Anal. Images Patterns*, Springer. pp. 95–107.
- [91] Le, T., Duan, Y., 2018. Pointgrid: A deep network for 3d shape understanding, in: *Proc. IEEE Conf. Comput. Vis. Pattern Recognit.*, pp. 9204–9214.
- [92] Lei, H., Akhtar, N., Mian, A., 2019. Octree guided cnn with spherical kernels for 3d point clouds, in: *Proc. IEEE Conf. Comput. Vis. Pattern Recognit.*, pp. 9631–9640.
- [93] Lei, H., Akhtar, N., Mian, A., 2020. Seggcn: Efficient 3d point cloud segmentation with fuzzy spherical kernel, in: *Proc. IEEE Conf. Comput. Vis. Pattern Recognit.*, pp. 11611–11620.
- [94] Lei, H., Akhtar, N., Mian, A., 2021. Spherical kernel for efficient graph convolution on 3d point clouds. *IEEE Trans. Pattern Anal. Mach. Intell.* 43, 3664–3680.
- [95] Lei, H., Akhtar, N., Shah, M., Mian, A., 2023. Mesh convolution with continuous filters for 3-d surface parsing. *IEEE Trans. Neural Netw. Learn. Syst.*, 1–15.
- [96] Li, G., Muller, M., Thabet, A., Ghanem, B., 2019a. Deepgcns: Can gcns go as deep as cnns?, in: *Proc. IEEE Int. Conf. Computer Vis.*, pp. 9267–9276.
- [97] Li, J., Chen, B.M., Hee Lee, G., 2018a. So-net: Self-organizing network for point cloud analysis, in: *Proc. IEEE Conf. Comput. Vis. Pattern Recognit.*, pp. 9397–9406.
- [98] Li, J., Dai, H., Han, H., Ding, Y., 2023. Mseg3d: Multi-modal 3d semantic segmentation for autonomous driving, in: *Proceedings of the IEEE/CVF conference on computer vision and pattern recognition*, pp. 21694–21704.
- [99] Li, J., Dong, Q., 2024. Density-guided semi-supervised 3d semantic segmentation with dual-space hardness sampling, in: *Proceedings of the IEEE/CVF Conference on Computer Vision and Pattern Recognition*, pp. 3260–3269.
- [100] Li, J., Zhang, X., Li, J., Liu, Y., Wang, J., 2020. Building and optimization of 3d semantic map based on lidar and camera fusion. *Neurocomputing* 409, 394–407.
- [101] Li, Y., Bu, R., Sun, M., Wu, W., Di, X., Chen, B., 2018b. Pointcnn: Convolution on x-transformed points. *Advances in Neural Information Processing Systems* 31, 820–830.
- [102] Li, Y., Ma, L., Zhong, Z., Cao, D., Li, J., 2019b. Tgnet: Geometric graph cnn on 3-d point cloud segmentation. *IEEE Trans. Geosci. Remote Sens.* 58, 3588–3600.
- [103] Li, Z., Gan, Y., Liang, X., Yu, Y., Cheng, H., Lin, L., 2016. Lstmcf: Unifying context modeling and fusion with lstms for rgb-d scene labeling, in: *Proc. Eur. Conf. on Comput. Vis.*, Springer. pp. 541–557.
- [104] Liang, Z., Li, Z., Xu, S., Tan, M., Jia, K., 2021. Instance segmentation in 3d scenes using semantic superpoint tree networks, in: *Proc. IEEE Int. Conf. Comput. Vis.*, pp. 2783–2792.
- [105] Liang, Z., Yang, M., Deng, L., Wang, C., Wang, B., 2019a. Hierarchical depthwise graph convolutional neural network for 3d semantic segmentation of point clouds, in: *Proc. IEEE Int. Conf. Robot. Autom.*, IEEE. pp. 8152–8158.
- [106] Liang, Z., Yang, M., Wang, C., 2019b. 3d graph embedding learning with a structure-aware loss function for point cloud semantic instance segmentation. arXiv preprint arXiv:1902.05247.

- [107] Lin, D., Chen, G., Cohen-Or, D., Heng, P., Huang, H., 2017. Cascaded feature network for semantic segmentation of rgb-d images, in: Proc. IEEE Int. Conf. Computer Vis., pp. 1311–1319.
- [108] Liu, C., Furukawa, Y., 2019. Masc: multi-scale affinity with sparse convolution for 3d instance segmentation. arXiv preprint arXiv:1902.04478 .
- [109] Liu, F., Li, S., Zhang, L., Zhou, C., Ye, R., Wang, Y., Lu, J., 2017. 3dcnn-dqn-rnn: A deep reinforcement learning framework for semantic parsing of large-scale 3d point clouds, in: Proc. IEEE Int. Conf. Computer Vis., pp. 5678–5687.
- [110] Liu, F., Shen, C., Lin, G., Reid, I., 2015. Learning depth from single monocular images using deep convolutional neural fields. IEEE Trans. Pattern Anal. Mach. Intell. 38, 2024–2039.
- [111] Liu, H., Wu, W., Wang, X., Qian, Y., 2018a. Rgb-d joint modelling with scene geometric information for indoor semantic segmentation. Multimed. Tools. Appl. 77, 22475–22488.
- [112] Liu, J., Wang, Y., Li, Y., Fu, J., Li, J., Lu, H., 2018b. Collaborative deconvolutional neural networks for joint depth estimation and semantic segmentation. IEEE Trans. Neural Netw. Learn. Syst. 29, 5655–5666.
- [113] Liu, W., Sun, J., Li, W., Hu, T., Wang, P., 2019a. Deep learning on point clouds and its application: A survey. Sensors 19, 4188.
- [114] Liu, Y., Yang, S., Li, B., Zhou, W., Xu, J., Li, H., Lu, Y., 2018c. Affinity derivation and graph merge for instance segmentation, in: Proc. Eur. Conf. on Comput. Vis., Springer. pp. 686–703.
- [115] Liu, Z., Tang, H., Lin, Y., Han, S., 2019b. Point-voxel cnn for efficient 3d deep learning, in: Advances in Neural Information Processing Systems, pp. 965–975.
- [116] Lowe, D.G., 2004. Distinctive image features from scale-invariant keypoints. Int. J. Comput. Vis. 60, 91–110.
- [117] Lu, J., Deng, J., Wang, C., He, J., Zhang, T., 2023. Query refinement transformer for 3d instance segmentation, in: Proceedings of the IEEE/CVF International Conference on Computer Vision, pp. 18516–18526.
- [118] Ma, X., Qin, C., You, H., Ran, H., Fu, Y., 2022. Rethinking network design and local geometry in point cloud: A simple residual mlp framework, in: International Conference on Learning Representations.
- [119] Ma, Y., Guo, Y., Liu, H., Lei, Y., Wen, G., 2020. Global context reasoning for semantic segmentation of 3d point clouds, in: Proc. IEEE Winter Conf. Appl. Comput. Vis., pp. 2931–2940.
- [120] Matrone, F., Grilli, E., Martini, M., Paolanti, M., Pierdicca, R., Remondino, F., 2020. Comparing machine and deep learning methods for large 3d heritage semantic segmentation. ISPRS International Journal of Geo-Information 9, 535.
- [121] Maturana, D., Scherer, S., 2015. Voxnet: A 3d convolutional neural network for real-time object recognition, in: Proc. IEEE Int. Conf. Intell. Rob. Syst., IEEE. pp. 922–928.
- [122] Meng, H., Gao, L., Lai, Y., Manocha, D., 2019. Vv-net: Voxel vae net with group convolutions for point cloud segmentation, in: Proc. IEEE Int. Conf. Computer Vis., pp. 8500–8508.
- [123] Meyer, G.P., Charland, J., Hegde, D., Laddha, A., Vallespi-Gonzalez, C., 2019. Sensor fusion for joint 3d object detection and semantic segmentation, in: Proc. IEEE Conf. Comput. Vis. Pattern Recognit. Worksh., pp. 0–0.
- [124] Milioto, A., Vizzo, I., Behley, J., Stachniss, C., 2019. Rangenet++: Fast and accurate lidar semantic segmentation, in: Proc. IEEE Int. Conf. Intell. Rob. Syst., IEEE. pp. 4213–4220.
- [125] Morton, G.M., 1966. A computer oriented geodetic data base and a new technique in file sequencing .
- [126] Mousavian, A., Pirsivash, H., Koščeká, J., 2016. Joint semantic segmentation and depth estimation with deep convolutional networks, in: Proc. Int. Conf. 3D Vis., IEEE. pp. 611–619.
- [127] Narita, G., Seno, T., Ishikawa, T., Kaji, Y., 2019. Panopticfusion: Online volumetric semantic mapping at the level of stuff and things. arXiv preprint arXiv:1903.01177 .
- [128] Naseer, M., Khan, S., Porikli, F., 2018. Indoor scene understanding in 2.5/3d for autonomous agents: A survey. IEEE Access 7, 1859–1887.
- [129] Ngo, T.D., Hua, B.S., Nguyen, K., 2023. Isbnet: a 3d point cloud instance segmentation network with instance-aware sampling and box-aware dynamic convolution, in: Proc. IEEE Conf. Comput. Vis. Pattern Recognit., pp. 13550–13559.
- [130] Park, C., Jeong, Y., Cho, M., Park, J., 2022. Fast point transformer, in: Proc. IEEE Conf. Comput. Vis. Pattern Recognit., pp. 16949–16958.
- [131] Park, J., Lee, S., Kim, S., Xiong, Y., Kim, H.J., 2023. Self-positioning point-based transformer for point cloud understanding, in: Proceedings of the IEEE/CVF conference on computer vision and pattern recognition, pp. 21814–21823.
- [132] Peng, B., Wu, X., Jiang, L., Chen, Y., Zhao, H., Tian, Z., Jia, J., 2024. Oa-cnns: Omni-adaptive sparse cnns for 3d semantic segmentation, in: Proceedings of the IEEE/CVF Conference on Computer Vision and Pattern Recognition, pp. 21305–21315.
- [133] Pham, Q., Hua, B., Nguyen, T., Yeung, S., 2019a. Real-time progressive 3d semantic segmentation for indoor scenes, in: Proc. IEEE Winter Conf. Appl. Comput. Vis., IEEE. pp. 1089–1098.
- [134] Pham, Q.H., Nguyen, T., Hua, B.S., Roig, G., Yeung, S.K., 2019b. Jsis3d: joint semantic-instance segmentation of 3d point clouds with multi-task pointwise networks and multi-value conditional random fields, in: Proc. IEEE Conf. Comput. Vis. Pattern Recognit., pp. 8827–8836.
- [135] Pierdicca, R., Paolanti, M., Matrone, F., Martini, M., Morbidoni, C., Malinverni, E.S., Frontoni, E., Lingua, A.M., 2020. Point cloud semantic segmentation using a deep learning framework for cultural heritage. Remote Sensing 12, 1005.
- [136] Qi, C.R., Su, H., Mo, K., Guibas, L.J., 2017a. Pointnet: Deep learning on point sets for 3d classification and segmentation, in: Proc. IEEE Conf. Comput. Vis. Pattern Recognit., pp. 652–660.
- [137] Qi, C.R., Yi, L., Su, H., Guibas, L.J., 2017b. Pointnet++: Deep hierarchical feature learning on point sets in a metric space. Advances in Neural Information Processing Systems 30, 5099–5108.
- [138] Qi, X., Liao, R., Jia, J., Fidler, S., Urtasun, R., 2017c. 3d graph neural networks for rgb-d semantic segmentation, in: Proc. IEEE Int. Conf. Computer Vis., pp. 5199–5208.
- [139] Qian, G., Li, Y., Peng, H., Mai, J., Hammoud, H.A.A.K., Elhoseiny, M., Ghanem, B., 2022. Pointnext: Revisiting pointnet++ with improved training and scaling strategies. arXiv preprint arXiv:2206.04670 .
- [140] Qin, T., Zheng, Y., Chen, T., Chen, Y., Su, Q., 2021. A light-weight semantic map for visual localization towards autonomous driving, in: 2021 IEEE international conference on robotics and automation (ICRA), IEEE. pp. 11248–11254.
- [141] Raj, A., Maturana, D., Scherer, S., 2015. Multi-scale convolutional architecture for semantic segmentation. Robotics Institute, Carnegie Mellon University, Tech. Rep. CMU-RITR-15-21 .
- [142] Ran, H., Liu, J., Wang, C., 2022. Surface representation for point clouds, in: Proc. IEEE Conf. Comput. Vis. Pattern Recognit., pp. 18942–18952.
- [143] Razani, R., Cheng, R., Li, E., Taghavi, E., Ren, Y., Bingbing, L., 2021. Gp-s3net: Graph-based panoptic sparse semantic segmentation network, in: Proceedings of the IEEE/CVF international conference on computer vision, pp. 16076–16085.
- [144] Rethage, D., Wald, J., Sturm, J., Navab, N., Tombari, F., 2018. Fully-convolutional point networks for large-scale point clouds, in: Proc. Eur. Conf. on Comput. Vis., Springer. pp. 596–611.
- [145] Riegler, G., Osman Ulusoy, A., Geiger, A., 2017. Octnet: Learning deep 3d representations at high resolutions, in: Proc. IEEE Conf. Comput. Vis. Pattern Recognit., pp. 3577–3586.
- [146] Riemenschneider, H., Bódis-Szomorú, A., Weissenberg, J., Van Gool, L., 2014. Learning where to classify in multi-view semantic segmentation, in: Proc. Eur. Conf. on Comput. Vis., Springer. pp. 516–532.

- [147] Rosu, R.A., Schütt, P., Quenzel, J., Behnke, S., 2019. Latticenet: Fast point cloud segmentation using permutohedral lattices. *arXiv preprint arXiv:1912.05905*.
- [148] Royndard, X., Deschaud, J., Goulette, F., 2018. Paris-lille-3d: A large and high-quality ground-truth urban point cloud dataset for automatic segmentation and classification. *Int. J. Rob. Res.* 37, 545–557.
- [149] Schult, J., Engelmann, F., Hermans, A., Litany, O., Tang, S., Leibe, B., 2023. Mask3d: Mask transformer for 3d semantic instance segmentation, in: 2023 IEEE International Conference on Robotics and Automation (ICRA), IEEE. pp. 8216–8223.
- [150] Shen, Y., Feng, C., Yang, Y., Tian, D., 2018. Mining point cloud local structures by kernel correlation and graph pooling, in: *Proc. IEEE Conf. Comput. Vis. Pattern Recognit.*, pp. 4548–4557.
- [151] Shi, H., Lin, G., Wang, H., Hung, T.Y., Wang, Z., 2020. Spsequencenet: Semantic segmentation network on 4d point clouds, in: *Proc. IEEE Conf. Comput. Vis. Pattern Recognit.*, pp. 4574–4583.
- [152] Shi, H., Wei, J., Li, R., Liu, F., Lin, G., 2022. Weakly supervised segmentation on outdoor 4d point clouds with temporal matching and spatial graph propagation, in: *Proc. IEEE Conf. Comput. Vis. Pattern Recognit.*, pp. 11840–11849.
- [153] Shi, H., Wei, J., Wang, H., Liu, F., Lin, G., 2024. Learning temporal variations for 4d point cloud segmentation. *International Journal of Computer Vision*, 1–15.
- [154] Shin, S., Zhou, K., Vankadari, M., Markham, A., Trigoni, N., 2024. Spherical mask: Coarse-to-fine 3d point cloud instance segmentation with spherical representation, in: *Proceedings of the IEEE/CVF Conference on Computer Vision and Pattern Recognition*, pp. 4060–4069.
- [155] Silberman, N., Fergus, R., 2011. Indoor scene segmentation using a structured light sensor, in: *Proc. IEEE Int. Conf. Computer Vis. Worksh.*, IEEE. pp. 601–608.
- [156] Silberman, N., Hoiem, D., Kohli, P., Fergus, R., 2012. Indoor segmentation and support inference from rgb-d images, in: *Proc. Eur. Conf. on Comput. Vis.*, Springer. pp. 746–760.
- [157] Simonovsky, M., Komodakis, N., 2017. Dynamic edge-conditioned filters in convolutional neural networks on graphs, in: *Proc. IEEE Conf. Comput. Vis. Pattern Recognit.*, pp. 3693–3702.
- [158] Song, S., Lichtenberg, S.P., Xiao, J., 2015. Sun rgb-d: A rgb-d scene understanding benchmark suite, in: *Proc. IEEE Conf. Comput. Vis. Pattern Recognit.*, pp. 567–576.
- [159] Song, Y., Chen, X., Li, J., Zhao, Q., 2017. Embedding 3d geometric features for rigid object part segmentation, in: *Proc. IEEE Int. Conf. Computer Vis.*, pp. 580–588.
- [160] Su, H., Jampani, V., Sun, D., Maji, S., Kalogerakis, E., Yang, M.H., Kautz, J., 2018. Splatnet: Sparse lattice networks for point cloud processing, in: *Proc. IEEE Conf. Comput. Vis. Pattern Recognit.*, pp. 2530–2539.
- [161] Su, H., Maji, S., Kalogerakis, E., Learned-Miller, E., 2015. Multi-view convolutional neural networks for 3d shape recognition, in: *Proc. IEEE Int. Conf. Computer Vis.*, pp. 945–953.
- [162] Su, Y., Xu, X., Jia, K., 2023. Weakly supervised 3d point cloud segmentation via multi-prototype learning. *IEEE Trans. Circuits Syst. Video Technol.* 33, 7723–7736.
- [163] Sun, J., Qing, C., Tan, J., Xu, X., 2023. Superpoint transformer for 3d scene instance segmentation, in: *Proceedings of the AAAI Conference on Artificial Intelligence*, pp. 2393–2401.
- [164] Tatarchenko, M., Park, J., Koltun, V., Zhou, Q.Y., 2018. Tangent convolutions for dense prediction in 3d, in: *Proc. IEEE Conf. Comput. Vis. Pattern Recognit.*, pp. 3887–3896.
- [165] Tchapmi, L., Choy, C., Armeni, I., Gwak, J., Savarese, S., 2017. Segcloud: Semantic segmentation of 3d point clouds, in: *Proc. Int. Conf. 3D Vis.*, IEEE. pp. 537–547.
- [166] Thomas, H., Qi, C.R., Deschaud, J.E., Marcotegui, B., Goulette, F., Guibas, L.J., 2019. Kpconv: Flexible and deformable convolution for point clouds, in: *Proc. IEEE Int. Conf. Computer Vis.*, pp. 6411–6420.
- [167] Thomas, H., Tsai, Y.H.H., Barfoot, T.D., Zhang, J., 2024. Kpconvx: Modernizing kernel point convolution with kernel attention, in: *Proceedings of the IEEE/CVF Conference on Computer Vision and Pattern Recognition*, pp. 5525–5535.
- [168] Valipour, S., Siam, M., Jagersand, M., Ray, N., 2017. Recurrent fully convolutional networks for video segmentation, in: *Proc. IEEE Winter Conf. Appl. Comput. Vis.*, IEEE. pp. 29–36.
- [169] Verma, N., Boyer, E., Verbeek, J., 2018. Feastnet: Feature-steered graph convolutions for 3d shape analysis, in: *Proc. IEEE Conf. Comput. Vis. Pattern Recognit.*, pp. 2598–2606.
- [170] Vu, T., Kim, K., Luu, T.M., Nguyen, T., Yoo, C.D., 2022. Softgroup for 3d instance segmentation on point clouds, in: *Proc. IEEE Conf. Comput. Vis. Pattern Recognit.*, pp. 2708–2717.
- [171] Wang, C., Samari, B., Siddiqi, K., 2018a. Local spectral graph convolution for point set feature learning, in: *Proc. Eur. Conf. on Comput. Vis.*, Springer. pp. 52–66.
- [172] Wang, J., Li, X., Sullivan, A., Abbott, L., Chen, S., 2022. Pointmotionnet: Point-wise motion learning for large-scale lidar point clouds sequences, in: *Proc. IEEE Conf. Comput. Vis. Pattern Recognit.*, pp. 4419–4428.
- [173] Wang, J., Tarrio, J., Agapito, L., Alcantarilla, P.F., Vakhitov, A., 2023. Semlaps: Real-time semantic mapping with latent prior networks and quasi-planar segmentation. *IEEE Robotics and Automation Letters*.
- [174] Wang, J., Wang, Z., Tao, D., See, S., Wang, G., 2016. Learning common and specific features for rgb-d semantic segmentation with deconvolutional networks, in: *Proc. Eur. Conf. on Comput. Vis.*, Springer. pp. 664–679.
- [175] Wang, P., Gan, Y., Shui, P., Yu, F., Zhang, Y., Chen, S., Sun, Z., 2018b. 3d shape segmentation via shape fully convolutional networks. *Comput. Graph.* 70, 128–139.
- [176] Wang, P., Shen, X., Lin, Z., Cohen, S., Price, B., Yuille, A., 2015. Towards unified depth and semantic prediction from a single image, in: *Proc. IEEE Conf. Comput. Vis. Pattern Recognit.*, pp. 2800–2809.
- [177] Wang, P.S., Liu, Y., Guo, Y.X., Sun, C.Y., Tong, X., 2017. Octree-based convolutional neural networks for 3d shape analysis. *ACM Trans. Graph.* 36, 1–11.
- [178] Wang, S., Suo, S., Ma, W.C., Pokrovsky, A., Urtasun, R., 2018c. Deep parametric continuous convolutional neural networks, in: *Proc. IEEE Conf. Comput. Vis. Pattern Recognit.*, pp. 2589–2597.
- [179] Wang, W., Neumann, U., 2018. Depth-aware cnn for rgb-d segmentation, in: *Proc. Eur. Conf. on Comput. Vis.*, Springer. pp. 135–150.
- [180] Wang, W., Yu, R., Huang, Q., Neumann, U., 2018d. Sgpn: Similarity group proposal network for 3d point cloud instance segmentation, in: *Proc. IEEE Conf. Comput. Vis. Pattern Recognit.*, pp. 2569–2578.
- [181] Wang, X., Liu, S., Shen, X., Shen, C., Jia, J., 2019a. Associatively segmenting instances and semantics in point clouds, in: *Proc. IEEE Conf. Comput. Vis. Pattern Recognit.*, pp. 4096–4105.
- [182] Wang, Y., Asafi, S., Van Kaick, O., Zhang, H., Cohen-Or, D., Chen, B., 2012. Active co-analysis of a set of shapes. *ACM Trans. Graph.* 31, 1–10.
- [183] Wang, Y., Shi, T., Yun, P., Tai, L., Liu, M., 2018e. Pointseg: Real-time semantic segmentation based on 3d lidar point cloud. *arXiv preprint arXiv:1807.06288*.
- [184] Wang, Y., Sun, Y., Liu, Z., Sarma, S.E., Bronstein, M.M., Solomon, J.M., 2019b. Dynamic graph cnn for learning on point clouds. *ACM Trans. Graph.* 38, 1–12.
- [185] Wang, Z., Lu, F., 2020. Voxsegnet: Volumetric cnns for semantic part segmentation of 3d shapes. *IEEE Trans. Vis. Comput. Graph.* 26, 2919–2930.
- [186] Wei, L.Y., 2008. Parallel poisson disk sampling. *ACM Trans. Graph.* 27, 1–9.
- [187] Wei, Y., Liu, H., Xie, T., Ke, Q., Guo, Y., 2022. Spatial-temporal transformer for 3d point cloud sequences, in: *Proc. IEEE Winter Conf. Appl. Comput. Vis.*, pp. 1171–1180.

- [188] Wei, Z., Chen, P., Yu, X., Li, G., Jiao, J., Han, Z., 2024. Semantic-aware sam for point-prompted instance segmentation, in: Proceedings of the IEEE/CVF Conference on Computer Vision and Pattern Recognition, pp. 3585–3594.
- [189] Wilson, J., Song, J., Fu, Y., Zhang, A., Capodiceci, A., Jayakumar, P., Barton, K., Ghaffari, M., 2022. Motionsc: Data set and network for real-time semantic mapping in dynamic environments. *IEEE Robotics and Automation Letters* 7, 8439–8446.
- [190] Wu, B., Wan, A., Yue, X., Keutzer, K., 2018a. Squeezeseg: Convolutional neural nets with recurrent crf for real-time road-object segmentation from 3d lidar point cloud, in: Proc. IEEE Int. Conf. Robot. Autom., IEEE. pp. 1887–1893.
- [191] Wu, B., Zhou, X., Zhao, S., Yue, X., Keutzer, K., 2019a. Squeeze-segv2: Improved model structure and unsupervised domain adaptation for road-object segmentation from a lidar point cloud, in: Proc. IEEE Int. Conf. Robot. Autom., IEEE. pp. 4376–4382.
- [192] Wu, C., Bi, X., Pfommer, J., Cebulla, A., Mangold, S., Beyerer, J., 2023. Sim2real transfer learning for point cloud segmentation: An industrial application case on autonomous disassembly, in: Proceedings of the IEEE/CVF Winter Conference on Applications of Computer Vision, pp. 4531–4540.
- [193] Wu, W., Qi, Z., Fuxin, L., 2019b. Pointconv: Deep convolutional networks on 3d point clouds, in: Proc. IEEE Conf. Comput. Vis. Pattern Recognit., pp. 9621–9630.
- [194] Wu, X., Jiang, L., Wang, P.S., Liu, Z., Liu, X., Qiao, Y., Ouyang, W., He, T., Zhao, H., 2024. Point transformer v3: Simpler faster stronger, in: Proceedings of the IEEE/CVF Conference on Computer Vision and Pattern Recognition, pp. 4840–4851.
- [195] Wu, X., Lao, Y., Jiang, L., Liu, X., Zhao, H., 2022a. Point transformer v2: Grouped vector attention and partition-based pooling. *Advances in Neural Information Processing Systems* 35, 33330–33342.
- [196] Wu, Y., Shi, M., Du, S., Lu, H., Cao, Z., Zhong, W., 2022b. 3d instances as 1d kernels, in: Proc. Eur. Conf. on Comput. Vis., Springer. pp. 235–252.
- [197] Wu, Y., Wu, Y., Gkioxari, G., Tian, Y., 2018b. Building generalizable agents with a realistic and rich 3d environment. *arXiv preprint arXiv:1801.02209*.
- [198] Wu, Z., Song, S., Khosla, A., Yu, F., Zhang, L., Tang, X., Xiao, J., 2015. 3d shapenets: A deep representation for volumetric shapes, in: Proc. IEEE Conf. Comput. Vis. Pattern Recognit., pp. 1912–1920.
- [199] Wu, Z., Zhou, Z., Allibert, G., Stolz, C., Démonceaux, C., Ma, C., 2022c. Transformer fusion for indoor rgb-d semantic segmentation. Available at SSRN 4251286.
- [200] Xiang, T., Zhang, C., Song, Y., Yu, J., Cai, W., 2021. Walk in the cloud: Learning curves for point clouds shape analysis, in: Proceedings of the IEEE/CVF international conference on computer vision, pp. 915–924.
- [201] Xiang, Y., Fox, D., 2017. Da-rnn: Semantic mapping with data associated recurrent neural networks. *arXiv preprint arXiv:1703.03098*.
- [202] Xiao, A., Huang, J., Guan, D., Zhang, X., Lu, S., Shao, L., 2023. Unsupervised point cloud representation learning with deep neural networks: A survey. *IEEE Trans. Pattern Anal. Mach. Intell.* 45, 11321–11339.
- [203] Xie, S., Gu, J., Guo, D., Qi, C.R., Guibas, L., Litany, O., 2020a. Pointcontrast: Unsupervised pre-training for 3d point cloud understanding, in: Computer Vision—ECCV 2020: 16th European Conference, Glasgow, UK, August 23–28, 2020, Proceedings, Part III 16, Springer. pp. 574–591.
- [204] Xie, Y., Tian, J., Zhu, X.X., 2020b. Linking points with labels in 3d: A review of point cloud semantic segmentation. *IEEE Trans. Geosci. Remote Sens.* 8, 38–59.
- [205] Xie, Z., Chen, J., Peng, B., 2020c. Point clouds learning with attention-based graph convolution networks. *Neurocomputing*.
- [206] Xu, C., Wu, B., Wang, Z., Zhan, W., Vajda, P., Keutzer, K., Tomizuka, M., 2020. Squeezesegv3: Spatially-adaptive convolution for efficient point-cloud segmentation. *arXiv preprint arXiv:2004.01803*.
- [207] Xu, H., Dong, M., Zhong, Z., 2017. Directionally convolutional networks for 3d shape segmentation, in: Proc. IEEE Int. Conf. Computer Vis., pp. 2698–2707.
- [208] Xu, M., Ding, R., Zhao, H., Qi, X., 2021. Paconv: Position adaptive convolution with dynamic kernel assembling on point clouds, in: Proc. IEEE Conf. Comput. Vis. Pattern Recognit., pp. 3173–3182.
- [209] Xu, Y., Fan, T., Xu, M., Zeng, L., Qiao, Y., 2018. Spidernn: Deep learning on point sets with parameterized convolutional filters, in: Proc. Eur. Conf. on Comput. Vis., Springer. pp. 87–102.
- [210] Yamazaki, K., Hanyu, T., Vo, K., Pham, T., Tran, M., Doretto, G., Nguyen, A., Le, N., 2024. Open-fusion: Real-time open-vocabulary 3d mapping and queryable scene representation, in: 2024 IEEE International Conference on Robotics and Automation (ICRA), IEEE. pp. 9411–9417.
- [211] Yan, X., Zheng, C., Li, Z., Wang, S., Cui, S., 2020. Pointasnl: Robust point clouds processing using nonlocal neural networks with adaptive sampling, in: Proc. IEEE Conf. Comput. Vis. Pattern Recognit., pp. 5589–5598.
- [212] Yang, B., Wang, J., Clark, R., Hu, Q., Wang, S., Markham, A., Trigoni, N., 2019. Learning object bounding boxes for 3d instance segmentation on point clouds. *Advances in Neural Information Processing Systems* 32, 6740–6749.
- [213] Yang, S., Hou, M., Li, S., 2024. Point cloud semantic segmentation of grotto scenes using the knowledge-guided deep learning method. *International Journal of Digital Earth* 17, 2385081.
- [214] Yang, Y., Xu, Y., Zhang, C., Xu, Z., Huang, J., 2022. Hierarchical vision transformer with channel attention for rgb-d image segmentation, in: Proceedings of the 4th International Symposium on Signal Processing Systems, pp. 68–73.
- [215] Ye, X., Li, J., Huang, H., Du, L., Zhang, X., 2018. 3d recurrent neural networks with context fusion for point cloud semantic segmentation, in: Proc. Eur. Conf. on Comput. Vis., Springer. pp. 403–417.
- [216] Yi, L., Gong, B., Funkhouser, T., 2021. Complete & label: A domain adaptation approach to semantic segmentation of lidar point clouds, in: Proceedings of the IEEE/CVF conference on computer vision and pattern recognition, pp. 15363–15373.
- [217] Yi, L., Kim, V., Ceylan, D., Shen, I., Yan, M., Su, H., Lu, C., Huang, Q., Sheffer, A., Guibas, L., 2016. A scalable active framework for region annotation in 3d shape collections. *ACM Trans. Graph.* 35, 1–12.
- [218] Yi, L., Su, H., Guo, X., Guibas, L.J., 2017. Syncspecnn: Synchronized spectral cnn for 3d shape segmentation, in: Proc. IEEE Conf. Comput. Vis. Pattern Recognit., pp. 2282–2290.
- [219] Yi, L., Zhao, W., Wang, H., Sung, M., Guibas, L.J., 2019. Gspn: Generative shape proposal network for 3d instance segmentation in point cloud, in: Proc. IEEE Conf. Comput. Vis. Pattern Recognit., pp. 3947–3956.
- [220] Ying, X., Chuah, M.C., 2022. Uctnet: Uncertainty-aware cross-modal transformer network for indoor rgb-d semantic segmentation, in: Proc. Eur. Conf. on Comput. Vis., Springer. pp. 20–37.
- [221] Yu, F., Liu, K., Zhang, Y., Zhu, C., Xu, K., 2019. Partnet: A recursive part decomposition network for fine-grained and hierarchical shape segmentation, in: Proc. IEEE Conf. Comput. Vis. Pattern Recognit., pp. 9491–9500.
- [222] Yuan, X., Shi, J., Gu, L., 2021. A review of deep learning methods for semantic segmentation of remote sensing imagery. *Expert Syst. Appl.* 169, 114417.
- [223] Yue, C., Wang, Y., Tang, X., Chen, Q., 2022. Drgcnn: Dynamic region graph convolutional neural network for point clouds. *Expert Syst. Appl.* 205, 117663.
- [224] Zeng, W., Gevers, T., 2018. 3dcontextnet: Kd tree guided hierarchical learning of point clouds using local and global contextual cues, in: Proc. Eur. Conf. on Comput. Vis., Springer. pp. 0–0.
- [225] Zhang, C., Wan, H., Shen, X., Wu, Z., 2022. Patchformer: An efficient point transformer with patch attention, in: Proc. IEEE Conf. Comput. Vis. Pattern Recognit., pp. 11799–11808.

- [226] Zhang, Y., Zhou, Z., David, P., Yue, X., Xi, Z., Gong, B., Foroosh, H., 2020. Polarnet: An improved grid representation for online lidar point clouds semantic segmentation, in: Proc. IEEE Conf. Comput. Vis. Pattern Recognit., pp. 9601–9610.
- [227] Zhang, Z., Yang, B., Wang, B., Li, B., 2023. Growsp: Unsupervised semantic segmentation of 3d point clouds, in: Proceedings of the IEEE/CVF Conference on Computer Vision and Pattern Recognition, pp. 17619–17629.
- [228] Zhao, H., Jiang, L., Fu, C.W., Jia, J., 2019a. Pointweb: Enhancing local neighborhood features for point cloud processing, in: Proc. IEEE Conf. Comput. Vis. Pattern Recognit., pp. 5565–5573.
- [229] Zhao, H., Jiang, L., Jia, J., Torr, P.H., Koltun, V., 2021a. Point transformer, in: Proc. IEEE Int. Conf. Comput. Vis., pp. 16259–16268.
- [230] Zhao, J., Liu, R., Hua, X., Yu, H., Zhao, J., Wang, X., Yang, J., 2024. Dsc-net: learning discriminative spatial contextual features for semantic segmentation of large-scale ancient architecture point clouds. *Heritage Science* 12, 274.
- [231] Zhao, N., Chua, T.S., Lee, G.H., 2021b. Few-shot 3d point cloud semantic segmentation, in: Proceedings of the IEEE/CVF Conference on Computer Vision and Pattern Recognition, pp. 8873–8882.
- [232] Zhao, S., Wang, Y., Li, B., Wu, B., Gao, Y., Xu, P., Darrell, T., Keutzer, K., 2021c. epointda: An end-to-end simulation-to-real domain adaptation framework for lidar point cloud segmentation, in: Proceedings of the AAAI Conference on Artificial Intelligence, pp. 3500–3509.
- [233] Zhao, Y., Birdal, T., Deng, H., Tombari, F., 2019b. 3d point capsule networks, in: Proc. IEEE Conf. Comput. Vis. Pattern Recognit., pp. 1009–1018.
- [234] Zhou, X., Liang, D., Xu, W., Zhu, X., Xu, Y., Zou, Z., Bai, X., 2024. Dynamic adapter meets prompt tuning: Parameter-efficient transfer learning for point cloud analysis, in: Proceedings of the IEEE/CVF Conference on Computer Vision and Pattern Recognition, pp. 14707–14717.